

**CO<sub>2</sub> seawater acidification by CCS-simulated leakage: Kinetic modelling of Zn, Pb, Cd, Ni, Cr, Cu and As release from contaminated estuarine sediment using pH-static leaching tests**

M.Camino Martín-Torre\*, Gema Ruiz, Berta Galán, Javier R. Viguri

Green Engineering & Resources Research Group (GER), Department of Chemistry and Process & Resources Engineering, ETSIIT, University of Cantabria, Avda. de los Castros s/n, 39005 Santander, Cantabria, Spain

\* Corresponding author. Tel.: +34 942 201583; fax: +34 942 206706

*E-mail address:* [martinmc@unican.es](mailto:martinmc@unican.es) (M.C. Martín-Torre)

**Highlights**

- Kinetic element release in a pH-static leaching test using CO<sub>2</sub> for acidification
- The model fits experimental release including the influence of Fe and other ions
- There is a leaching simulation over time under acidic scenarios up to pH=6
- CO<sub>2</sub> and HNO<sub>3</sub> acidifications lead to different kinetics during element release
- The generalised model proposed here is also useful for areas contaminated by iron

**Keywords:** Kinetic modelling; CO<sub>2</sub> acidification; contaminant release; sediment; pH-static leaching; Fe influence

**Abstract**

A modified pH-dependent leaching test with continuous pH control that employed CO<sub>2</sub> to acidify a seawater-sediment mixture is used to address Zn, Pb, Cd, Ni, Cr, Cu and As release from contaminated estuarine sediments under the influence of acidification

processes. Long-term (480 h) leaching experiments at pH values of 7.0, 6.5 and 6.0 are performed. The different evolutionary patterns of the redox potential and Fe release at pH=6 with respect to the other pH values shows the need to assess the influence of the initial Fe content in seawater upon elemental release.

Hence, assays at pH=6.0 are conducted using natural seawater with Fe concentrations between 9.02 and 153 µg/L. A set of in-series reactions for trace elements, Fe and other ions associated with Fe is proposed to model a Fe/multi-ion-dependent mechanism for trace metal release. The maximum concentration of each contaminant that can be released from the sediment and the kinetic parameters of the proposed model are completed for the studied pH values, for good consistency between the experimental and simulated mobilisation of each studied element.

## 1. INTRODUCTION

Carbon capture and storage (CCS) in geological formations is one of the most promising strategies for curbing global climate change (IPCC, 2014). One of the primary risks in the case of ocean storage technology is the potential direct leakage of CO<sub>2</sub> gas or CO<sub>2</sub> dissolved in seawater, which provokes a decrease in the pH of the medium. This acidification might mobilise contaminants from marine and estuarine sediments (Rodríguez-Romero et al., 2014; Ardelan et al., 2009).

Laboratory leaching tests allow for the assessment of contaminant releases under different scenarios and conditions. Column leaching tests (Bateman et al., 2005; Frye et al., 2012; Lawter et al., 2016; Payán et al., 2012a) and batch or semi-batch leaching

tests (Ardelan and Steinnes, 2010; Ardelan et al., 2009; de Orte et al., 2014; Kirsch et al., 2014; Little and Jackson, 2010; Lu et al., 2010; Payán et al., 2012b) have been performed to assess elemental mobilisation from different types of matrices such as sediments, sandstones or rocks when the addition of CO<sub>2</sub> decreases the pH of the medium.

The release of experimental contaminants from sediments and rocks by using different leaching tests to mimic the effects of potential CO<sub>2</sub> leakages has been studied before. Equilibrium conditions have been modelled using geochemical software such as PHREEQC or Visual MINTEQ (de Orte et al., 2014a; Martín-Torre et al., 2015a), whereas simulations for the period before equilibrium is achieved have been performed using reactive transport models as performed with the TOUGHREACT code (Zheng et al., 2016; Zheng et al., 2009) or PHREEQC (Cahill and Jakobsen, 2015).

Reactive transport models combine mineral dissolution/precipitation, aqueous complexation, acid-base, redox, cation exchange and surface complexation processes. Therefore, the use of this type of models for simulating contaminant mobilisation implies that the modelled has knowledge of the different characteristics of the solid matrix under study, such as crystalline phases, that are usually not possible to know in the case of sediments because of their great complexity and low contaminant concentrations. Moreover, the need to pre-treat the sediment sample complicates the determination of element speciation in a sensitive manner.

The pH is one of the variables that most influences the mobility and availability of inorganic contaminants from solid matrices (Coz et al., 2007), and thus, pH-dependent

leaching tests seem to be an appropriate assay for assessing its influence. Standard or modified pH-dependent leaching tests with continuous pH control such as CEN/TS 14997 (2015) have been widely used to evaluate the release of contaminants from soil and sediments (Cappuyns and Swennen, 2005; Cappuyns et al 2004a,b; Centioli et al., 2008; Horckmans et al., 2007; Shtiza et al., 2009; Van Herreweghe et al., 2002).

To study the release of contaminants that occurs when environmental conditions in marine and estuarine media vary, a modified pH-dependent leaching test with continuous pH control has been previously performed to assess the contaminants released from contaminated sediment when a total mixture of sediment-seawater is acidified by nitric acid ( $\text{HNO}_3$ ) (Martín-Torre et al., 2015b). Based on these experimental results, a kinetic mathematical model has been proposed to obtain the generalised kinetic constants of the studied elemental release. Owing to the experimental difficulties involved in characterising the sediment and the many chemical reactions that occurred during the process, global phenomena rather than specific reactions have been considered.

It is known that inorganic contaminants, primarily metals and metalloids, are largely affected by acidification processes (Basallote et al., 2014), and that their effects on marine organisms are higher when using  $\text{CO}_2$  gas than mineral acids (Ishimatsu et al., 2004; Kikkawa et al., 2004). Hence, the performance of a pH-dependent leaching test with  $\text{CO}_2$  gas for acidification and the subsequent assessment and modelling of the triggered contaminant mobilisation from sediment would be useful for a CCS technology impact assessment.

The aim of the present work is to obtain, analyse and simulate the experimental release of Zn, Pb, Cd, Ni, Cr, Cu and As from contaminated marine sediments during the pH-static leaching test with continuous pH control by using seawater as a leaching liquid and CO<sub>2</sub> gas to acidify the medium. The kinetic behaviour of Zn, Pb, Cd, Ni, Cr, Cu and As is studied by using long-term experiments lasting 480 hours at pH values of 7.0, 6.5 and 6.0. The influence of the Fe content of the seawater on the redox potential evolution and elemental release is highlighted at pH=6.0 because of the different evolution of these parameters with respect to the experimental data obtained at pH values of 7.0 and 6.5.

Starting with the mathematical model by Martín-Torre et al. (2015b) in which HNO<sub>3</sub> acidification was initially proposed, a modified kinetic model is proposed here to explain the behaviour of long-term experimental data at different pH values and different Fe concentrations in seawater. The generalised kinetic expression and its kinetic parameters are obtained to fit the experimental and modelled release of the elements.

## **2. MATERIALS AND METHODS**

The selected estuarine sediment samples were collected in the Suances estuary (Cantabrian region, northern Spain), which is a representative area for a possible CCS (BOE, 2008). As explained in detail in Martín-Torre et al. (2015b), surface sediment (0-5 cm) and its initial water content was collected using a plastic paddle, and it was sieved through a 2 mm plastic mesh to remove the gravel fraction. Afterwards, the sediment was homogenised and frozen in plastic bags until use.

An X-ray diffraction analysis (Siemens D5000 diffractometer) using Cu K $\alpha$  radiation and operating at 30 mA and 50 kV was used to determine the crystalline phases of the selected sediment (Payán et al. 2012b). The total sediment content was determined by an external laboratory (Activation Laboratories, Canada). The As and Cr contents were measured by Instrumental Neutron Activation Analysis (INAA) and the Cd, Cu, Ni, Pb and Zn contents were analysed by Total Digestion-Inductively Coupled Plasma/ Optical Emission Spectrometry (TD-ICP/OES) method.

The results of the sediment characterisation are explained in more detail in Martín-Torre et al. (2015b), but they are described briefly in Table 1.

Table 1. Principal crystalline phases, redox potential and trace element concentrations of the studied sediment

Principal crystalline phases	Trace element	Content (mg/kg)
Quartz	Zn	5220 $\pm$ 140
Aluminium oxide	Pb	564 $\pm$ 2.22
Calcite	Cd	12.6 $\pm$ 0.732
Dolomite	Ni	36 $\pm$ 1.86
	Cu	48 $\pm$ 3.43
	Cr	72 $\pm$ 5.31
	As	59 $\pm$ 1.39
Redox potential (mV): -150 $\pm$ 37		

The entire Cantabrian region and the Suances estuary in particular was an important mining area, with a considerable number of iron ore mines and abandoned landfills containing solid mining wastes. Therefore, the presence of this metal in rivers and effluents that lead in the estuary and its accumulation in sediment is appreciable. Therefore, the concentration of iron in the area from which the seawater is taken should be influenced by tides and other atmospheric conditions. To prevent large variations in the concentration determinations, the seawater was chemically analysed by using

inductively coupled plasma-mass spectrometry (ICP-MS) equipment in helium collision mode according to the same procedure that was used for the sample leachates, prior to use. Table 2 lists the average elemental concentrations in the seawater that was used in the leaching assays at pH=7.0, 6.5 and 6.0. Seawater samples with iron concentrations ( $[\text{Fe}]_{\text{seawater}}$ ) of 9.02, 46.1 and  $\mu\text{g/L}$  were sampled at the same place that the sediment was taken from but under different natural conditions of tide, meteorology and season.

Table 2. Concentration of the studied elements and redox potential in the seawater leachant

Element	Content ( $\mu\text{g/L}$ )
As	$2.58 \pm 0.981$
Cd	$0.204 \pm 0.0797$
Cr	$0.920 \pm 0.631$
Cu	$2.46 \pm 1.49$
Ni	$1.21 \pm 1.37$
Pb	$0.929 \pm 0.727$
Zn	$11.6 \pm 8.21$
Fe	$6.45 \pm 2.91$
Redox potential (mV)	$160 \pm 16.0$

The experimental equipment consisted of a glass-made 2-L jacketed vessel, a temperature controller (Polyscience) and a system for maintaining a constant pH (Fig. 1). In this study, a pH controller (AT Control systems) with an electrode that was suitable for samples containing suspended solids was used; it was accurate to 0.01 pH units and was calibrated against standard solutions. This device was used to monitor the pH and inject pure  $\text{CO}_2$  bubbles into the suspension as needed, with a permitted hysteresis of 0.1 pH units. When the suspension reached the required pH, the gas supply was automatically stopped.

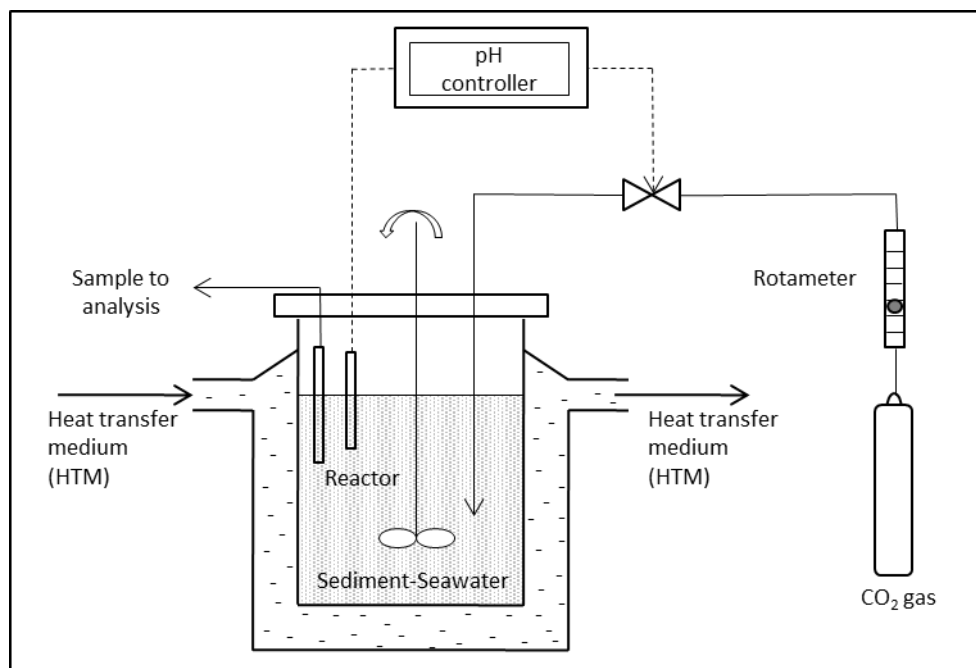


Fig. 1. Experimental equipment used in the pH-static leaching test with continuous pH control.

Seawater and sediment were placed in a reactor with an L/S ratio of 10, considering the moisture of the sediment (51.26%). To make a homogenised mixture at the beginning of the assay, the reactor was shaken for 15 minutes at the natural pH before starting the CO<sub>2</sub> addition (CO<sub>2</sub> supplied by AL Air Liquide España, S.A., Zamudio, Vizcaya, País Vasco, Spain). In this work, the studied pH values are 7.0, 6.5 and 6.0. It was not possible to achieve lower pH values because of the high buffering capacity of the sediment-seawater system (Martín-Torre et al., 2015a). Additionally, an assay without pH control was conducted to observe the pH evolution over time.

The pH-static leaching tests conducted in this work lasted almost 480 hours to achieve near-equilibrium conditions, which were not obtained over shorter assay durations (Martín-Torre et al., 2015b). Nevertheless, the assay at pH=7.0 lasts 264 hours, when the consumption of the buffer capacity of the mixture makes the pH uncontrollable. The experiments were performed in duplicate. Samples at 0, 0.5 h, 1 h, 3 h, 6 h, 12 h, 24 h,



48 h, 72 h, 96 h and afterwards for every 48 hours were taken using a syringe and without stopping the mixing. The redox potential (Eh) of the leachate was measured using a Basic 20 pH metre (Crison) with a special electrode for samples containing suspended solids; each sample was filtered through a 0.45- $\mu$ m pore size nitrocellulose filtration membrane and acidified to determine the concentrations of Fe, Zn, Pb, Cd, Ni, Cr, Cu and As. The corresponding amount of solids was put back in the medium to maintain a constant L/S ratio during the whole assay.

The elemental concentrations were determined by an external laboratory (Mass Spectrometry Unit, University of Oviedo, Spain) using Agilent 7500CE inductively coupled plasma-mass spectrometry (ICP-MS) equipment in helium-collision mode (Agilent Technologies, California, EEUU). The samples were diluted (1:20) with HNO<sub>3</sub> (VWR International, Fontenay-sous-Bois, France) 1% prior to analysis, and Rh was added as an internal standard to correct for the eventual signal drift during analysis. The metal concentrations were calculated using external calibration with internal standard correction. The certified reference material NASS-5 (Seawater reference material for trace metals, NRCC (Ontario, Canada)) was spiked with the elements at two different concentration levels of 1 and 10  $\mu$ g/L. The certified reference material and the two spiked concentrations were measured every 6 samples as a quality control. The detection limits for the elements under study (Fe, Zn, Pb, Cd, Ni, Cr, Cu and As) were 0.79; 0.75; 0.02; 0.06; 0.23; 0.03; 0.21 and 0.16  $\mu$ g/L, respectively. Prior to the experiments, all the sampling and laboratory material was precleaned, acid-washed (10% HNO<sub>3</sub>), and rinsed with Milli-Q water (Direct-Q 5 UV, Merck Millipore, USA).

The modelling of this study and the estimation of the corresponding parameters are completed using Aspen Custom Modeler software (Bedford, Massachusetts, USA) which solves rigorous models and simultaneously estimates parameters. The adjustment of the model parameters was performed using an NL2SOL algorithm for the least-square minimization of the deviation between the experimental and theoretical data.

### **3. RESULTS**

#### **3.1. Evolution of redox potential and Fe release at pH=7.0, 6.5 and 6.0**

The evolution of the redox potential ( $E_h$ ) over time is followed in all the assays. Similar to the findings of Cappuyns and Swennen (2005), this evolution is as useful as the exact values when considering that the measured value is a mixed redox potential. It cannot be a true equilibrium potential because of the different redox couples in the sediment and the slow kinetics of redox reactions (Sigg, 2000).

To compare the evolution of the redox potential at the different pH values under study better, Fig. 2 shows the evolution of the redox variation ( $E_h - E_{h,0}$ ) over time. During the first 30-60 minutes of the assay there is a rapid increase in the  $E_h$  value, possibly because of the dissolution of major ions from the sediment. After this initial increase, a common trend is observed for pH=7.0 and 6.5. In these cases, the  $E_h$  value increases from  $t=1$  h until  $t=50-72$  h. Afterwards, the value of this parameter remains almost constant.

At pH=6.0 and the Fe concentration in the selected seawater ( $[Fe]_{\text{seawater}}$ ) of  $9.02 \mu\text{g/L}$ , the  $E_h$  value shows an irregular and different time behaviour it decreases from 1 to 12 hours. Afterwards, it remains almost constant until 48 h, when a rapid increase begins.

After a maximum  $E_h$  of 96 h, a decrease occurs. There is a subsequent increase until 192 h, when it remains almost constant until the end of the assay.

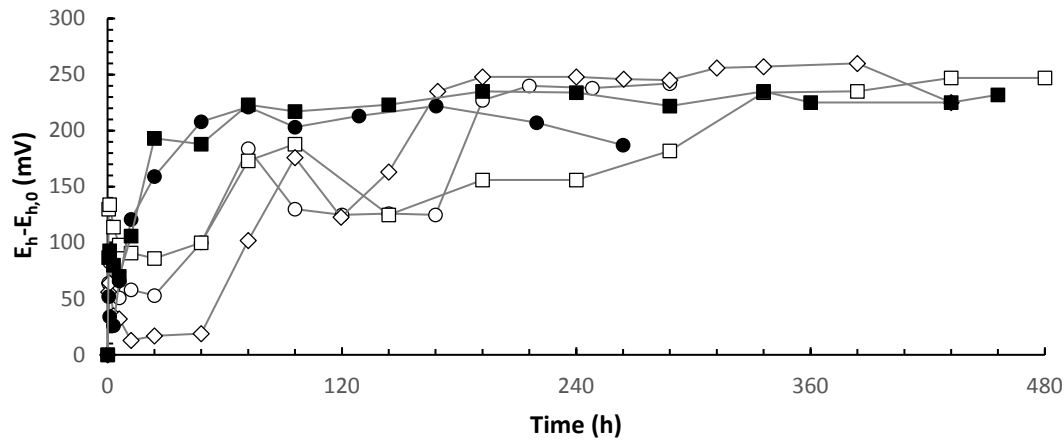


Fig. 2. Evolution of redox variation (mV) over time in pH-static leaching tests.  $E_{h,0}$  and  $E_h$  are the redox potentials at  $t=0$  h and  $t=t$ , respectively. ● pH=7; ■ pH=6.5; ◇ pH=6.0,  $[Fe]_{\text{seawater}}=9.02 \mu\text{g/L}$ ; ○ pH=6.0,  $[Fe]_{\text{seawater}}=46.1 \mu\text{g/L}$ ; and □ pH=6.0,  $[Fe]_{\text{seawater}}=153 \mu\text{g/L}$ . Connecting lines were added for clarity.

As shown in Fig. 3 a and b, at pH values of 7.0 and 6.5, the dissolved Fe concentration increases during the first three hours because of the mixing of the wet sediment with the seawater and possibly because of the oxidation and later release of different iron compounds. Afterwards, there is a decrease in the dissolved Fe concentration as a consequence of the Fe(II) to Fe(III) oxidation and the subsequent precipitation of Fe(III), which is much less soluble than Fe(II). When Fe(III) precipitates, it might form various compounds such as Fe oxyhydroxides (Appelo et al., 1999; Wang et al., 2016). A minimum value of approximately  $10 \mu\text{g/L}$ , which remains constant until the end of the assay, is achieved at  $t=24$  h when the pH is 7.0 and at 96 hours at pH=6.5.

The release of Fe at pH=6.0 and  $[Fe]_{\text{seawater}}= 9.02 \mu\text{g/L}$  (Fig. 3 c) is higher than it is at more neutral pH values because of its higher solubility at lower pH values (Johnston et al., 2016). Moreover, the experimental results at pH=6.0 indicate that high concentrations of Fe remain dissolved until 48 hours of the assay has passed, most

likely because of the slower oxidation of Fe(II) to Fe(III) at pH=6.0. This finding is completely consistent with previous studies showing that the rate constant of Fe(II) oxidation increases at higher pH values as well as in the presence of  $\text{HCO}_3^-$  ions (Millero and Izaguirre, 1989; Millero et al., 1987). The concentration of  $\text{HCO}_3^-$  at pH values of 7.0 and 6.5 (0.90 and 0.82 molar fraction, respectively) is higher than it is at pH=6.0 (0.6 molar fraction) (Payán et al., 2013). In coinciding with the high increase of the  $E_h$  value from 48 to 96 h, the dissolved Fe concentration decreases because of its oxidation to Fe(III) and its subsequent precipitation. A low Fe release, from 40 to 60  $\mu\text{g/L}$ , is maintained from  $t=192$  h to the end of the assay. This final dissolved concentration is higher at pH=6.0 than at more neutral pH values, likely because of the increase of in the Fe solubility at lower pH values.

The different behaviour of both parameters ( $E_h$  and Fe release) at pH=6.0 leads us to assess the influence of the initial Fe concentration in the seawater on the elemental release and to consider it as an important variable in leaching tests at pH=6.0.

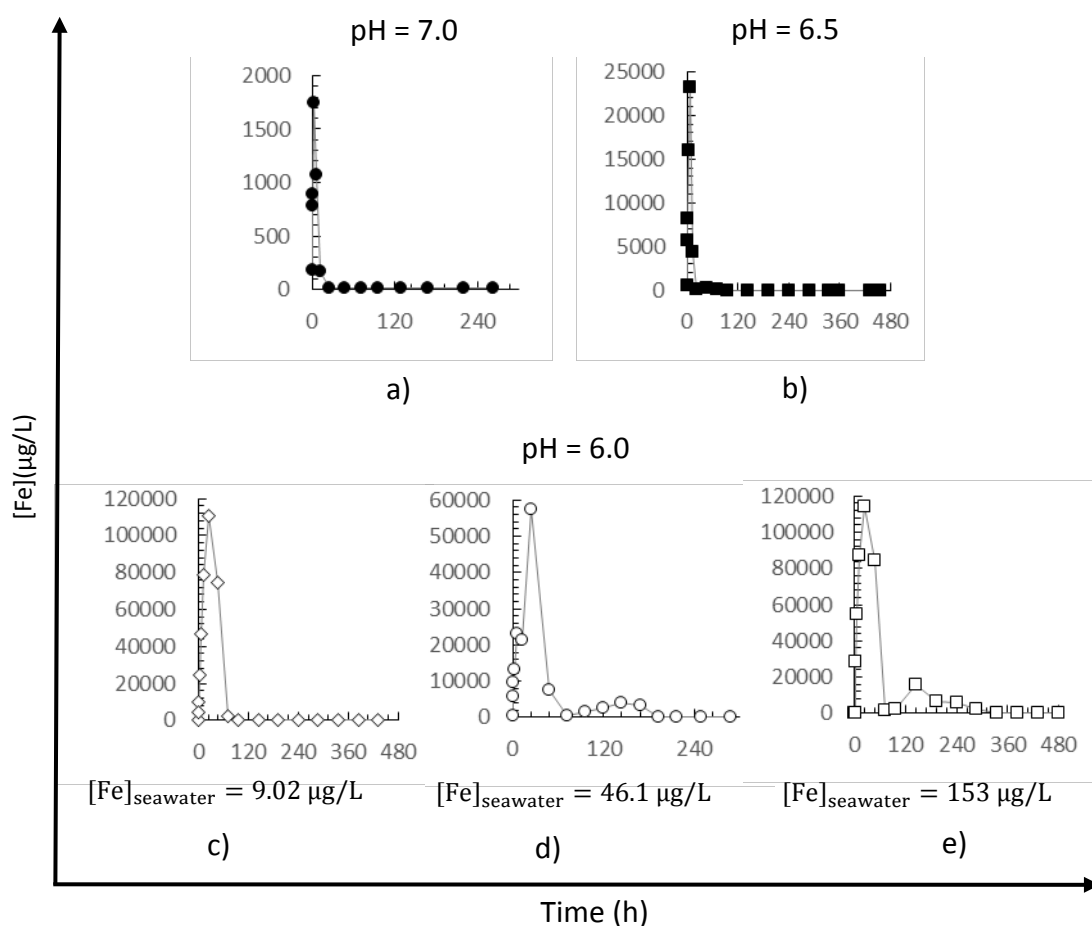


Fig. 3. Fe release ( $\mu\text{g/L}$ ) over time in pH-static leaching tests:  $\bullet$  pH=7;  $\blacksquare$  pH=6.5;  $\diamond$  pH=6.0,  $[\text{Fe}]_{\text{seawater}}=9.02 \mu\text{g/L}$ ;  $\circ$  pH=6.0,  $[\text{Fe}]_{\text{seawater}}=46.1 \mu\text{g/L}$ ; and  $\square$  pH=6.0,  $[\text{Fe}]_{\text{seawater}}=153 \mu\text{g/L}$ . Connecting lines were added for clarity.

### 3.2. Evolution of redox potential and Fe release at pH=6.0 using seawater with different Fe content

In accounting for the fact that the Fe concentration of the selected seawater from the studied estuarine area fluctuates because of local tides and atmospheric conditions, assays at pH=6.0 are conducted using seawater with higher Fe concentrations, namely 46.1 and 153  $\mu\text{g/L}$ , and lower  $E_h$  values of 61 and 116 mV, respectively. The concentrations of the other studied elements do not present as much variation, and they fall within the concentration range shown in Table 2.

In Fig. 2, the value of  $E_h$  increases in the assays conducted at pH=6.0 when using seawater with higher concentrations of Fe are also shown. During the first 24 hours of the assay, the evolution of the  $E_h$  of the three assays that were performed at pH=6.0 follows the same pattern: the increase during the first half hour is followed by a slight decrease and a plateau that lasts until 24 h when the  $[Fe]_{\text{seawater}}=46.1 \mu\text{g/L}$  or 48 hours in the other two cases. This difference might be more strongly influenced by the concentration of the major ions that are present in the seawater and the heterogeneity of the sediment rather than by the Fe content of the seawater. When the plateau ends, a rapid increase occurs until 72-96 h, depending on the experiment. At  $t=72$  h and  $[Fe]_{\text{seawater}}=46.1 \mu\text{g/L}$ , the  $E_h$  begins to decrease and a plateau is observed until  $t=168$  h. At the lowest and highest  $[Fe]_{\text{seawater}}$ , the decrease begins at 96 h and it lasts from 96 to 144 h in the case of  $[Fe]_{\text{seawater}}=153 \mu\text{g/L}$ . Afterwards, there is an increase, which is less pronounced at higher Fe concentrations in the seawater, which ends in a constant value that is maintained until the end of the assay. The time at which the redox potential begins to remain constant seems to depend on the Fe content, because at the higher seawater Fe concentration, a constant  $E_h$  value is achieved later (192 h, 216 h and 432 h).

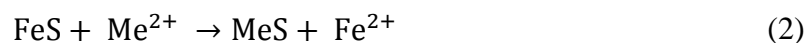
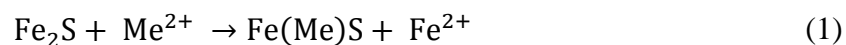
In all the assays conducted at pH=6, high Fe concentrations are in dissolution during the first 24 or 48 hours (Fig. 3 c, d and e). Afterwards, the precipitation of Fe(III) decreases the dissolved Fe concentration, and a minimum release is observed at 72 h ( $[Fe]_{\text{seawater}} = 46.1$  and  $153 \mu\text{g/L}$ ) or 96 h when  $[Fe]_{\text{seawater}}=9.02 \mu\text{g/L}$ . In assays with  $[Fe]_{\text{seawater}}$  values of 46.1 and  $153 \mu\text{g/L}$ , an increase in the Fe mobilisation is observed at 168 and 288 h, respectively; it is more pronounced at the highest Fe concentration in the initial seawater. Once the dissolved Fe concentration decreases after the second peak, likely

because of the Fe(II) oxidation and later precipitation of Fe(III), similar Fe release values are obtained at the end of the three assays that were performed at pH=6.0 (36.5±8.5 µg/L).

The fact that there is a second dissolved Fe concentration peak suggests a mobilisation that could be induced by different phenomena such as the destabilisation of Fe(III) oxyhydroxides or ionic competition and displacement reactions.

The destabilisation of Fe(III) oxyhydroxides could be caused by their reductive dissolution (Root et al., 2007). In this case, the abiotic reactions promoted by organic compounds present in the medium and H<sub>2</sub>S might provoke this reductive dissolution (Hering and Stumm, 1990; Schwertmann, 1991; Thamdrup, 2000). Luther III et al. (1992) identify acidification as one of the different impacts that cause iron oxyhydroxides to become unstable. H<sub>2</sub>S could be formed when Fe-sulphides are dissolved, and S<sup>2-</sup> reacts with protons from the acidification (Cappuyns and Swennen, 2005). In the presence of sulphides, destabilised iron oxyhydroxides are converted into iron sulphides (Salomons, 1995; Luther III et al., 1992) that might be oxidised and released into the medium.

Iron monosulphides are partially soluble in water, with higher solubility at lower pH values, whereas other metal monosulphides are less soluble than Fe monosulphides. Hence, the displacement of Fe from monosulphides occurred as well as the inclusion of other divalent metals in iron monosulphides, as shown in Eqs. 1 and 2 respectively, could be the cause of an increase in the concentration of dissolved Fe<sup>2+</sup> (Di Toro et al., 1990; Morse and Arakaki, 1993; Wong et al., 2013).



Ionic competition is a phenomenon that might be occurring constantly because of the huge number of ions present in the medium, because seawater was used as well as the acidification caused by CO<sub>2</sub> gas. In contrast to the assays at pH=6.0 with HNO<sub>3</sub> by Martín-Torre et al. (2015b), in this study the displacement reactions might be an important phenomenon because CO<sub>2</sub> gas was used to acidify the mixture. The use of this gas instead of HNO<sub>3</sub> to acidify- the mixture affects the different equilibria present in the suspension, and the newly formed ions could highly influence the release of the studied contaminants (Tokoro et al., 2010).

### 3.3. Trace element release

The average value of the experimental results obtained for the release of Zn, Pb, Cd, Ni, As, Cu and Cr from the pH-static leaching test and the error bars between both replicates are shown in Fig. 4. The relative error between both replicates under the same leaching conditions is lower than 20% for any of the studied contaminants. Moreover, the relative error of more than 85% of the experimental data for Zn, Pb, Cd, Ni and As is lower than 10%. Most of the experimental data from the Cr and Cu release show errors between 10% and 20%, likely as a consequence of their low mobilisation from the sediment in any of the studied conditions. The release of Cr is lower than 2 µg/L and does not present a clear trend over time. Something similar occurs in the case of Cu in that its release does not indicate a clear pattern and its dissolved concentration is lower



than 10 µg/L in all of the studied scenarios with respect to the pH and Fe concentrations.

The release of Ni does not present any initial delay in any of the assays. Moreover, after an initial rapid release, a near-equilibrium condition is reached after 300 h of the assay at pH values of 7.0 and 6.5. It is necessary to extend the experiment from 432-480 h to reach this condition in assays that were conducted pH=6.0. As shown here, in comparing the three assays at this most acidic pH value, lower Fe concentrations in seawater cause a faster mobilisation of Ni as well as a higher dissolved Ni concentration under the near-equilibrium condition.

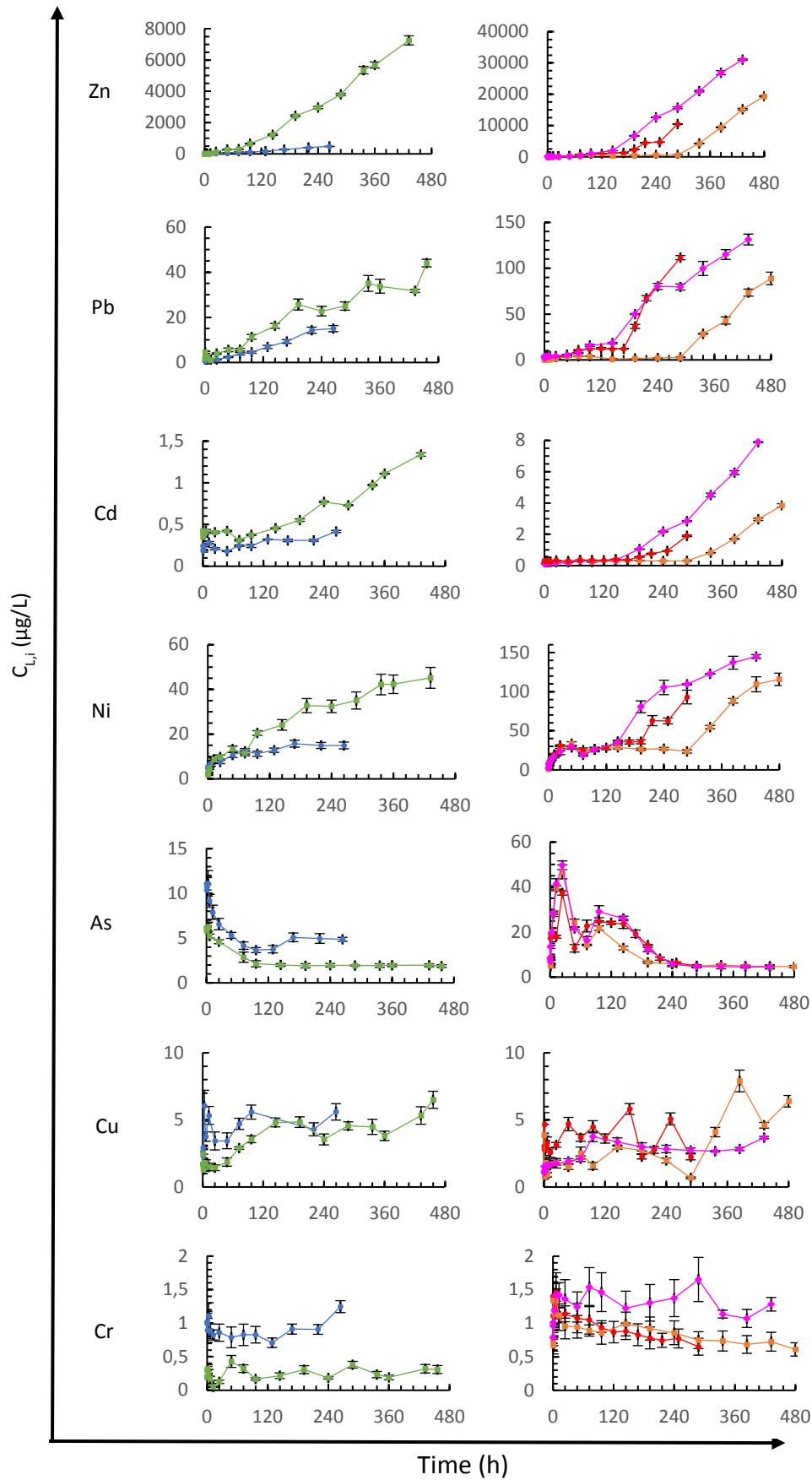


Fig. 4. Elemental release over time in all assays. • pH=7.0; ■ pH=6.5; ♦ pH=6.0,  $[\text{Fe}]_{\text{seawater}}=9.02 \mu\text{g/L}$ ; • pH=6.0,  $[\text{Fe}]_{\text{seawater}}=46.1 \mu\text{g/L}$ ; and ■ pH=6.0,  $[\text{Fe}]_{\text{seawater}}=153 \mu\text{g/L}$ . Connecting lines were added for clarity. Error bars are also shown.

Regarding Cd, Pb and Zn mobilisation, an initial delay is observed that might be the consequence of the association of these metals with sulphur and the slow oxidation kinetics of these metal sulphides during the assay (Cappuyns and Swennen, 2008; Ho et al., 2012). This finding is supported by the evolution of the pH over time in the assay without pH control as shown in Fig. 5. Without CO<sub>2</sub> addition, the acidification of the medium that was observed during the first 65 h of assay, might be caused by the H<sup>+</sup> released from the oxidation reactions of reduced compounds such as sulphides (Cappuyns and Swennen, 2005; Eggleton and Thomas, 2004; Hwang et al., 2011). At pH=6.0, higher concentrations of Fe in the seawater cause longer delays in the release of these metals as a consequence of the higher solubility of Fe monosulphides than the cation monosulphides, which favours the precipitation of dissolved metal ions (Di Toro et al., 1990; Morse and Arakaki, 1993) at the same time that Fe<sup>2+</sup> is released (Eq. 1 and 2). Moreover, the delay caused by the different solubility products might also be influenced by ionic competition to form compounds with other ions in the medium, such as CO<sub>3</sub><sup>2-</sup>, SO<sub>4</sub><sup>2-</sup> or Cl<sup>-</sup> (Millero, 2009; Millero et al., 1995; Wong et al., 2013).

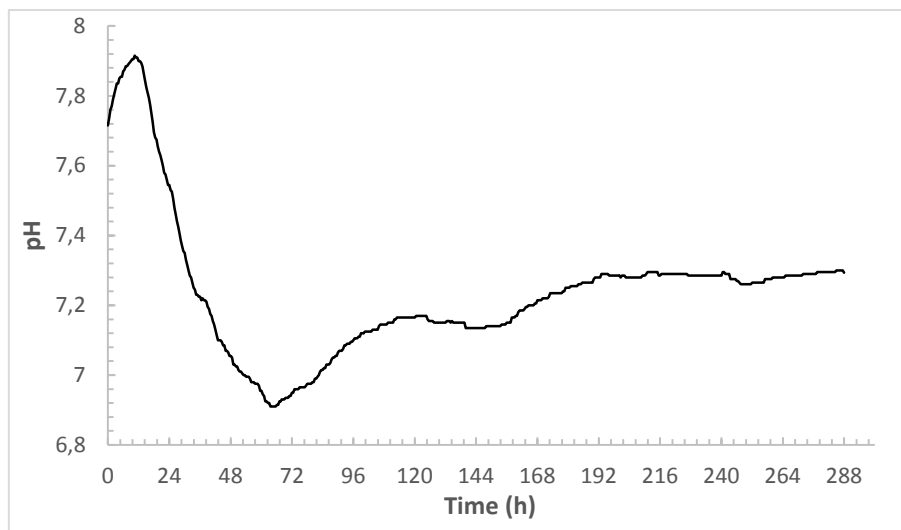


Fig. 5. pH evolution over time in the leaching test without pH control.

After an initial rapid release of As from the sediment, which became more pronounced at more neutral pH values, there is a decrease in the As concentration. The removal of this element from the solution has been widely believed to be caused by the coprecipitation and adsorption provoked by the production of iron oxyhydroxides (Cappuyns et al., 2005; Omoregie et al., 2013; Wallmann et al., 1996; Zhang et al., 2007); therefore, the oxidation rate of Fe(II) highly influences the time over which the oxyanion As remains in solution. Hence, at the most acidic pH value in the study, the presence of dissolved As is longer than that of the other two pH values under study. Moreover, As precipitation as trace metal arsenates represents a potential mechanism that contributes to this decrease (Vaca-Escobar et al., 2015). In the case of pH=6.0, after a minimum dissolved concentration of approximately 48-72 h, the mobilisation of As increases. This mobilisation might be a consequence of the destabilisation of Fe(III) oxyhydroxides, and the As might be adsorbed. The lower adsorbing capacity of iron sulphides, which are formed with the destabilisation of Fe(III) oxyhydroxides, causes an increase in the dissolved As concentration (Salomons, 1995). Moreover, sorbed As could be released after being displaced by the action of other oxyacids such as

phosphate, sulphate, carbonate, bicarbonate and silicate (Appelo et al., 2002; Arai et al., 2014; Jain and Loppert, 2000; Meng et al., 2002, 2000).

#### **4. MODELLING AND DISCUSSION**

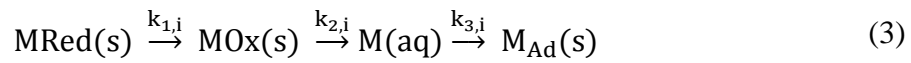
The pH-static leaching test used here allows for the study of elemental release from contaminated sediment as a function of pH and time. Modelling the obtained experimental results is useful for assessing the evolution of contaminant over time at the pH values of interest.

Owing to the impossibility of performing a rigorous characterisation of all the species present in the sediment, the difficulties involved in analysing the major seawater ions mobilised from the sediment and the high number of chemical reactions that occurred during elemental release, simplified kinetic models that consider general reaction schemes to interpret contaminant release from sediments are usually proposed (Martín-Torre et al., 2015b).

Therefore, generalised mathematical models are useful for studying contaminant release and for determining the principal processes that influence their mobilisation, without specifying all the phenomena that occurred within the sediment. The proposed mathematical model is not applied to the experimental results of Cu and Cr because their release over time does not present a clear trend, and it is very low, at lower than 10 µg/L in all cases.

##### **4.1. Generalised kinetic model as applied to Zn, Pb, Cd, Ni, Cr, Cu and As**

The kinetic model proposed in Martín-Torre et al. (2015b) for HNO<sub>3</sub> acidification, is used here. This model considers that the contaminant (M) is associated with an oxidised fraction (MOx) and with a reduced fraction (MRed) of the sediment that must be oxidised before the release of the element. Moreover, it includes the adsorption or precipitation of the released element through a third reaction in series. The reaction scheme and mass balances, when considering first-order reactions, are shown in Eqs. 3-7.



$$\frac{d[\text{MRed}]_i}{dt} = -k_{1,i} [\text{MRed}]_i \quad (4)$$

$$\frac{d[\text{MOx}]_i}{dt} = k_{1,i} [\text{MRed}]_i - k_{2,i} [\text{MOx}]_i \quad (5)$$

$$\frac{d[\text{M}]_i}{dt} = k_{2,i} [\text{MOx}]_i - k_{3,i} [\text{M}]_i \quad (6)$$

$$\frac{d[\text{MAd}]_i}{dt} = k_{3,i} [\text{M}]_i \quad (7)$$

where [MRed]<sub>i</sub>, [MOx]<sub>i</sub>, [M]<sub>i</sub> and [MAd]<sub>i</sub> are the concentrations of element i in the reduced sediment fraction, the oxidised sediment fraction, the aqueous phase and in the adsorbed or precipitated phase, respectively. The k<sub>j,i</sub> are the rate coefficients of element i in reaction j (oxidation, release or adsorption/precipitation), and t is the reaction time.

The integral equation of the set from Eqs. 4-7 is shown in Eq. 8.

$$\begin{aligned}
\frac{LS}{1000} [M]_i = & \left( \frac{k_{1,i} k_{2,i} [MRed]_{i,0}}{(k_{2,i} - k_{1,i}) (k_{3,i} - k_{1,i})} \right) \exp(-k_{1,i}t) \\
& + \left( \frac{k_{1,i} k_{2,i} [MRed]_{i,0}}{(k_{1,i} - k_{2,i}) (k_{3,i} - k_{2,i})} \right. \\
& \left. - \frac{k_{2,i} [MOx]_{i,0}}{(k_{2,i} - k_{3,i})} \right) \exp(-k_{2,i}t) \\
& + \left( \frac{LS [M]_{i,0}}{1000} + \frac{k_{2,i} [MOx]_{i,0}}{(k_{2,i} - k_{3,i})} \right. \\
& \left. + \frac{k_{2,i} k_{1,i} [MRed]_{i,0}}{(k_{1,i} - k_{3,i}) (k_{2,i} - k_{3,i})} \right) \exp(-k_{3,i}t)
\end{aligned} \tag{8}$$

450

451 where LS corresponds to the Liquid/Solid ratio of the experiment,  $[M]_{i,0}$ , which is  
452 expressed in units of  $\mu\text{g/L}$ , is the concentration of element  $i$  in the liquid at  $t = 0$  and  
453  $[MRed]_{i,0}$  and  $[MOx]_{i,0}$  are the maximum concentration as expressed in  $\text{mg/kg}$ , of  
454 element  $i$  that can be released from the reduced and oxidised fractions of the sediment  
455 respectively.

456

457 The resolution of the model implies the estimation of the rate coefficients and the initial  
458 concentrations of each contaminant  $i$  in the oxidised and reduced fractions ( $[MOx]_{i,0}$   
459 and  $[MRed]_{i,0}$ , respectively) based on the experimental results. The experimental and  
460 simulated results obtained at pH values of 7.0, 6.5 and 6 at  $[\text{Fe}]_{\text{seawater}} = 9.02 \mu\text{g/L}$  are  
461 shown in Fig. 6 and 7, and the initial concentrations are listed in Table 3. To better  
462 represent the elemental release, a dimensionless quotient (Eqs. 9-10) is represented over  
463 time.

$$x_i = \frac{[M]_i - [M]_{i,0}}{\frac{[MS]_{i,0}}{LS}} \tag{9}$$

$$[MS]_{i,0} = [MOx]_{i,0} + [MRed]_{i,0} \quad (10)$$

where  $[M]_i$  is the dissolved concentration of the element  $i$  at any time (in units of  $\mu\text{g/L}$ ),  $[M]_{i,0}$  is the dissolved concentration of the element  $i$  at  $t = 0$  (in units of  $\mu\text{g/L}$ ),  $[MRed]_{i,0}$  and  $[MOx]_{i,0}$  are the maximum concentrations of the element  $i$  that can be leached from the reduced and oxidised fractions of the sediment, respectively (in units of  $\text{mg/kg}$ ),  $[MS]_{i,0}$  is the maximum concentration of element  $i$  that can be released from the sediment (in units of  $\text{mg/kg}$ ) and  $LS$  is the Liquid/Solid ratio of the experiment (in  $\text{L/kg}$ ).

Higher concentrations are released from the reduced fraction than from the oxidised fraction, except in the case of  $\text{Ni}$ , because of the initial reduced state of the sediment. In the case of  $\text{Cd}$ , its concentration in the oxidised fraction is zero.

Table 4 lists the kinetic rate coefficients of the reactions ( $k_{j,i}$ ). According to the experimental results obtained here, the third adsorption or precipitation reaction is only included in the case of  $\text{As}$ . For the  $\text{pH}$  values under study, a good fit between experimental and simulated release concentrations is indicated by the percentage variation-explained values ( $R^2$ ) of 99.4 ( $\text{pH} = 7.0$ ), 99.6 ( $\text{pH} = 6.5$ ) and 98.3 ( $\text{pH} = 6.0$ ) and  $[\text{Fe}]_{\text{seawater}} = 9.02 \mu\text{g/L}$ .

Using the model published in Martín-Torre et al. (2015b), the simulated results for  $\text{Zn}$ ,  $\text{Pb}$ ,  $\text{Cd}$ ,  $\text{Ni}$  and  $\text{As}$  fit more poorly with the experimental data at  $\text{pH} = 6.0$  than at the higher  $\text{pH}$  values, as shown in Fig. 7 with dashed lines for the three assays at this  $\text{pH}$  value. Among the different assays at  $\text{pH} = 6.0$ , the better fit is obtained at the lowest concentration of seawater  $\text{Fe}$  ( $9.02 \mu\text{g/L}$ ), and it seems that the initial concentration of



Fe in the seawater highly influences the characteristics of the medium, modifying the release behaviour of the contaminants. The experimental release of Zn, Pb and Cd at pH=6.0 present a longer delay than that simulated with this model. This delay in the release could be a consequence of the displacement reactions because of the higher solubility of the Fe(II) compounds at the most acidic pH value under study. The studied trace elements, except As, present a rapid release once Fe is removed from the aqueous phase. Hence, a modified mathematical model that considers the initial Fe concentration, its release and its precipitation is proposed.

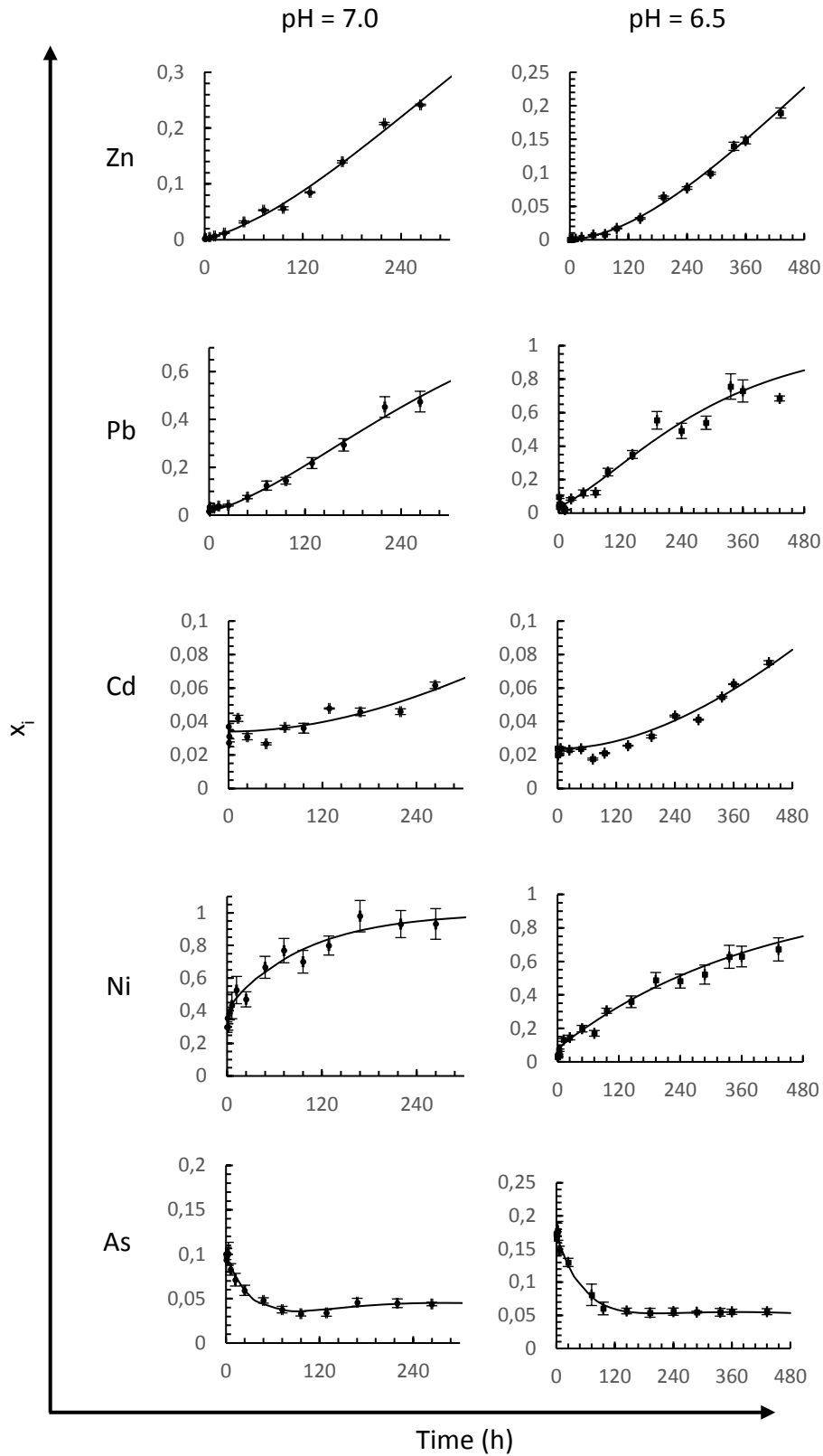


Fig. 6. Trace element release  $x_i = \{[M]_i - [M]_{i,0}\} / \{[MS]_{i,0} / LS\}$  over time at pH values of 7.0 and 6.5, where  $i$  is the trace element,  $[M]_i$  is the dissolved concentration of the element  $i$ ,  $[M]_{i,0}$  is the dissolved concentration of the element  $i$  at  $t = 0$  and  $[MS]_{i,0}$  is the maximum concentration of the element that can be released from the sediment. The experimental release ( $\bullet$  pH=7;  $\blacksquare$  pH=6.5), error bars and simulated curves using the model by Martín-Torre et al. (2015b) (—) are represented.

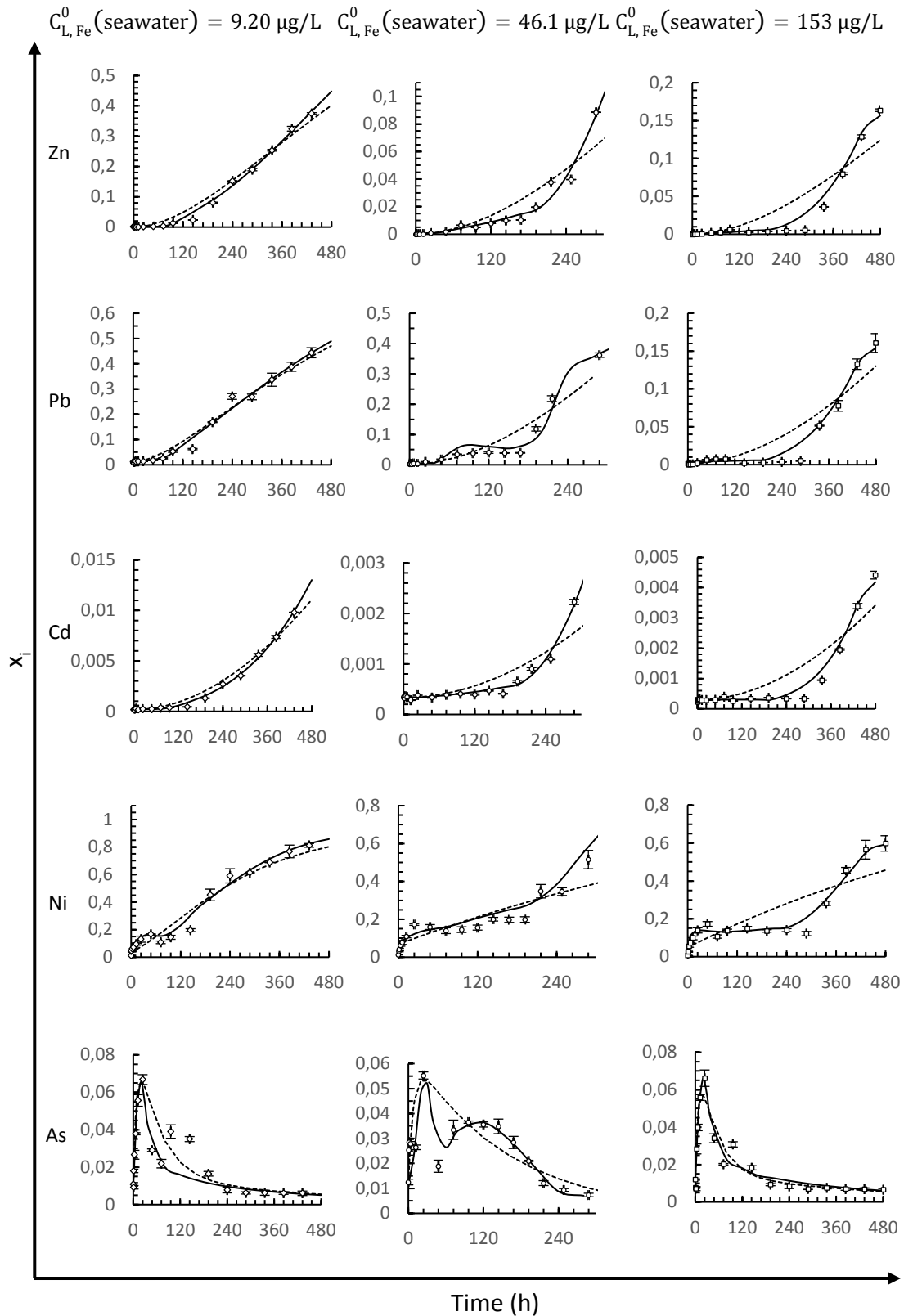


Fig. 7. Trace element release ( $x_i = \{[M]_i - [M]_{i,0}\} / \{[MS]_{i,0} / LS\}$ ) over time at pH=6.0, where i is the trace element,  $[M]_i$  is the dissolved concentration of the element i,  $[M]_{i,0}$  is the dissolved concentration of the element i at  $t = 0$  and  $[MS]_{i,0}$  is the maximum concentration of the element that can be released from the sediment. Experimental release ( $\diamond$  pH=6.0,  $[Fe]_{\text{seawater}}=9.02 \mu\text{g/L}$ ;  $\circ$  pH=6.0,  $[Fe]_{\text{seawater}}=46.1 \mu\text{g/L}$ ; and  $\square$  pH=6.0,  $[Fe]_{\text{seawater}}=153 \mu\text{g/L}$ ), error bars and simulated curves are represented: --- Martín-Torre et al. (2015b) model; and — modified model

Table 3. Estimated values of the maximum concentrations that can be released from the reduced and oxidised fractions of the sediment, ( $[MRed]_{i,0}$  and  $[MOx]_{i,0}$  respectively), as expressed in units of mg/kg.

Assay		Contaminant									
pH	[Fe] <sub>seawater</sub> (µg/L)	Zn		Pb		Cd		Ni		As	
		[ZnRed] <sub>0</sub>	[ZnOx] <sub>0</sub>	[PbRed] <sub>0</sub>	[PbOx] <sub>0</sub>	[CdRed] <sub>0</sub>	[CdOx] <sub>0</sub>	[NiRed] <sub>0</sub>	[NiOx] <sub>0</sub>	[AsRed] <sub>0</sub>	[AsOx] <sub>0</sub>
<u>Martín-Torre et al. (2015b) model</u>											
7.0	6.80	17.6	2.06	0.280	0.0359	0.0676	0	0.0908	0.280	0.971	0.136
6.5	3.50	373	10.8	0.390	0.0733	0.178	0	0.635	0.390	0.298	0.0557
6.0*	9.02	828	0	2.96	0	8.06	0	1.14	2.96	5.01	2.43
<u>Modified model for pH=6</u>											
6.0	46.1	1150	33.9	3.07	0.012	8.53	0	1.65	3.07	4.37	7.70
6.0	153	1110	70.6	5.11	0.424	8.71	0	1.082	5.11	4.40	2.37

521

522 \*Estimated concentrations at pH=6 and  $[Fe]_{seawater}=9.02 \mu g/L$  take the same value when using the model by Martín-Torre et al. (2015b) and the modified model at pH=6.

523

524

525

526

527

528

Table 4. Estimated kinetic rate coefficients for each contaminant in all the assays.

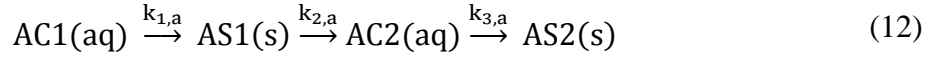
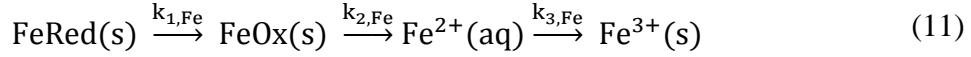
Assay		Contaminant						
pH	[Fe] <sub>seawater</sub> ( $\mu\text{g/L}$ )	$k_{j,i}$ ( $\text{h}^{-1}$ )	Zn	Pb	Cd	Ni	As	
<u>Martín-Torre et al. (2015b)</u> <u>model</u>								
7.0	6.80	$k_{1,i}$	$3.10 \cdot 10^{-3}$	$5.02 \cdot 10^{-3}$	$7.77 \cdot 10^{-3}$	$9.95 \cdot 10^{-3}$	$3.54 \cdot 10^{-3}$	
		$k_{2,i}$	$3.30 \cdot 10^{-3}$	$6.34 \cdot 10^{-3}$	$1.09 \cdot 10^{-3}$	$3.06 \cdot 10^{-3}$	$3.62 \cdot 10^{-3}$	
		$k_{3,i}$	0	0	0	0	$2.92 \cdot 10^{-2}$	
6.5	3.50	$k_{1,i}$	$1.96 \cdot 10^{-3}$	$4.64 \cdot 10^{-3}$	$6.41 \cdot 10^{-3}$	$2.54 \cdot 10^{-3}$	$2.08 \cdot 10^{-3}$	
		$k_{2,i}$	$1.70 \cdot 10^{-3}$	$8.60 \cdot 10^{-3}$	$1.04 \cdot 10^{-3}$	$2.91 \cdot 10^{-1}$	$2.86 \cdot 10^{-3}$	
		$k_{3,i}$	0	0	0	0	$1.64 \cdot 10^{-2}$	
6.0	9.02	$k_{1,i}$	$2.30 \cdot 10^{-3}$	$1.60 \cdot 10^{-3}$	$3.01 \cdot 10^{-4}$	$7.69 \cdot 10^{-3}$	$2.18 \cdot 10^{-3}$	
		$k_{2,i}$	$3.68 \cdot 10^{-3}$	$1.09 \cdot 10^{-3}$	$3.46 \cdot 10^{-4}$	$5.88 \cdot 10^{-3}$	$1.74 \cdot 10^{-2}$	
		$k_{3,i}$	0	0	0	0	$1.15 \cdot 10^{-1}$	
<u>Modified model for pH=6</u>								
6.0	9.02	$k_{1,i}$	$2.30 \cdot 10^{-3}$	$1.60 \cdot 10^{-3}$	$3.01 \cdot 10^{-4}$	$7.69 \cdot 10^{-3}$	$2.18 \cdot 10^{-3}$	
		$k_{2,i}$	$k_{2,i}^0$	$5.28 \cdot 10^{-4}$	$4.36 \cdot 10^{-3}$	$2.57 \cdot 10^{-5}$	0	$1.14 \cdot 10^{-2}$
			$k_{2,i}^1$	$1.74 \cdot 10^{-5}$	$4.08 \cdot 10^{-5}$	$1.65 \cdot 10^{-6}$	$4.05 \cdot 10^{-5}$	$2.34 \cdot 10^{-3}$
			$k_{2,i}^2$	---	0	---	$2.03 \cdot 10^{-3}$	0
		$k_{3,i}$	0	0	0	0	$1.15 \cdot 10^{-1}$	
6.0	46.1	$k_{1,i}$	$2.30 \cdot 10^{-3}$	$1.60 \cdot 10^{-3}$	$3.01 \cdot 10^{-4}$	$7.69 \cdot 10^{-3}$	$2.18 \cdot 10^{-3}$	
		$k_{2,i}$	$k_{2,i}^0$	$4.87 \cdot 10^{-4}$	$2.46 \cdot 10^{-3}$	$4.89 \cdot 10^{-5}$	$1.59 \cdot 10^{-3}$	$1.25 \cdot 10^{-3}$
			$k_{2,i}^1$	$4.28 \cdot 10^{-6}$	$8.91 \cdot 10^{-4}$	$6.62 \cdot 10^{-7}$	$1.57 \cdot 10^{-6}$	$5.29 \cdot 10^{-4}$
			$k_{2,i}^2$	---	$3.91 \cdot 10^{-4}$	---	$2.47 \cdot 10^{-3}$	$5.57 \cdot 10^{-3}$
		$k_{3,i}$	0	0	0	0	$1.15 \cdot 10^{-1}$	
6.0	153	$k_{1,i}$	$2.30 \cdot 10^{-3}$	$1.60 \cdot 10^{-3}$	$3.01 \cdot 10^{-4}$	$7.69 \cdot 10^{-3}$	$2.18 \cdot 10^{-3}$	
		$k_{2,i}$	$k_{2,i}^0$	$1.19 \cdot 10^{-4}$	$8.38 \cdot 10^{-6}$	0	0	$1.14 \cdot 10^{-2}$
			$k_{2,i}^1$	$1.01 \cdot 10^{-6}$	$1.58 \cdot 10^{-6}$	$1.78 \cdot 10^{-7}$	$3.50 \cdot 10^{-6}$	$4.35 \cdot 10^{-3}$
			$k_{2,i}^2$	---	$3.91 \cdot 10^{-4}$	---	$5.41 \cdot 10^{-4}$	0
		$k_{3,i}$	0	0	0	0	$1.15 \cdot 10^{-1}$	

## 4.2. Kinetic model of Fe release

When using the kinetic model by Martín-Torre et al. (2015b), the good fit between the experimental and simulated Fe release at pH values of 7.0 and 6.5 is shown in Fig. 8. Moreover, the Fe concentrations in the reduced and oxidised fractions, or  $[\text{FeRed}]_0$  and  $[\text{FeOx}]_0$ , respectively, and the rate coefficients for the simulated Fe release at these pH values are listed in Table 5.

However, this model cannot explain the behaviour of Fe at the most acidic pH value under study. At pH=6.0, the simulated curves that employ this model explain the release of Fe within short periods but do not explain its decrease, nor is the second peak observed in Fe mobilisation (dashed curves in Fig. 8).

More complex kinetic schemes, which always consider first-order reactions with respect to Fe, have been tested to find a mathematical model that better predicts the behaviour of this element at pH=6.0. The possibility that Fe is released directly from the reduced fraction was considered; iron sulphides such as pyrite could be released into the medium without being oxidised. Another hypothesis was that most of the dissolved Fe precipitates took the form of Fe(III), whereas the rest of it precipitates as Fe(II) before being released again to the medium; afterwards, this re-dissolved Fe could precipitate as Fe(III). These kinetically Fe-dependent schemes do not improve the previous fitting, and so we propose that there is a dependency between the Fe release and the presence of other ions in association. Therefore, a model that includes the kinetics of ions associated with Fe is introduced. The global model of Fe consists of two series of reactions in parallel (Eqs. 11 and 12) and includes the influence of other ions on the release of Fe.



Eq. 11 considers that reduced Fe should be oxidised before being released from the sediment into the medium, and that dissolved Fe precipitates as Fe(III) whereas Eq. 12 represents an additional scheme for ions that are associated with Fe. Ions that are associated with Fe in solution (AC1) could precipitate with Fe (AS1) and be released together (AC2) and precipitated (AS2) because of the different solubility of products from the compounds present in the medium. This scheme is feasible because of the high concentration of ions dissolved in the seawater-sediment system and the ionic interactions associated with this situation.

The association between Fe and these ions is taken into account by assuming that the release and precipitation rate coefficients, namely  $k_{2,\text{Fe}}$  and  $k_{3,\text{Fe}}$ , depend on the dissolved concentration of these ions through Eqs. 13 and 14.

$$k_{2,\text{Fe}} = k_{2,\text{Fe}}^0 + k_{2,\text{Fe}}^1 x_A \quad (13)$$

$$k_{3,\text{Fe}} = k_{3,\text{Fe}}^0 + k_{3,\text{Fe}}^1 (1 - x_A) \quad (14)$$

where  $k_{2,\text{Fe}}^0$ ,  $k_{2,\text{Fe}}^1$ ,  $k_{3,\text{Fe}}^0$  and  $k_{3,\text{Fe}}^1$  are kinetic rate coefficients and  $x_A$  is the fraction of ions released from the sediment, as calculated as  $x_A = \frac{\text{AC2} - \text{AC1}_0}{\text{AC}_{\text{max}}}$ . AC2 refers to the concentration of ions released with Fe, AC1<sub>0</sub> is the concentration of seawater ions associated with Fe and AC<sub>max</sub> is the maximum concentration of ions associated with Fe in the aqueous phase.

In Fig. 8, the simulated curves at pH=6.0 are shown using a continuous line. The proposed model fits well with the experimental data, including the second peak observed at the higher Fe concentrations in the selected seawater. The good fit is corroborated by the percentage variation-explained values ( $R^2$ ) (99.3, 95.8 and 96.1 when the Fe concentrations of the seawater are 9.02, 46.1 and 153  $\mu\text{g/L}$ , respectively). Additionally, Table 5 lists the maximum concentration of Fe that can be released from each fraction of the sediment and kinetic rate coefficients using the latter model.

This more complex model has been applied to the Fe release at pH values of 7.0 and 6.5 without obtaining an improvement in the simulated results. The global percentage variation-explained value of 97.8 and a relative standard deviation of 0.325 could be concluded for the Fe release model at the pH values and Fe seawater concentrations under study.

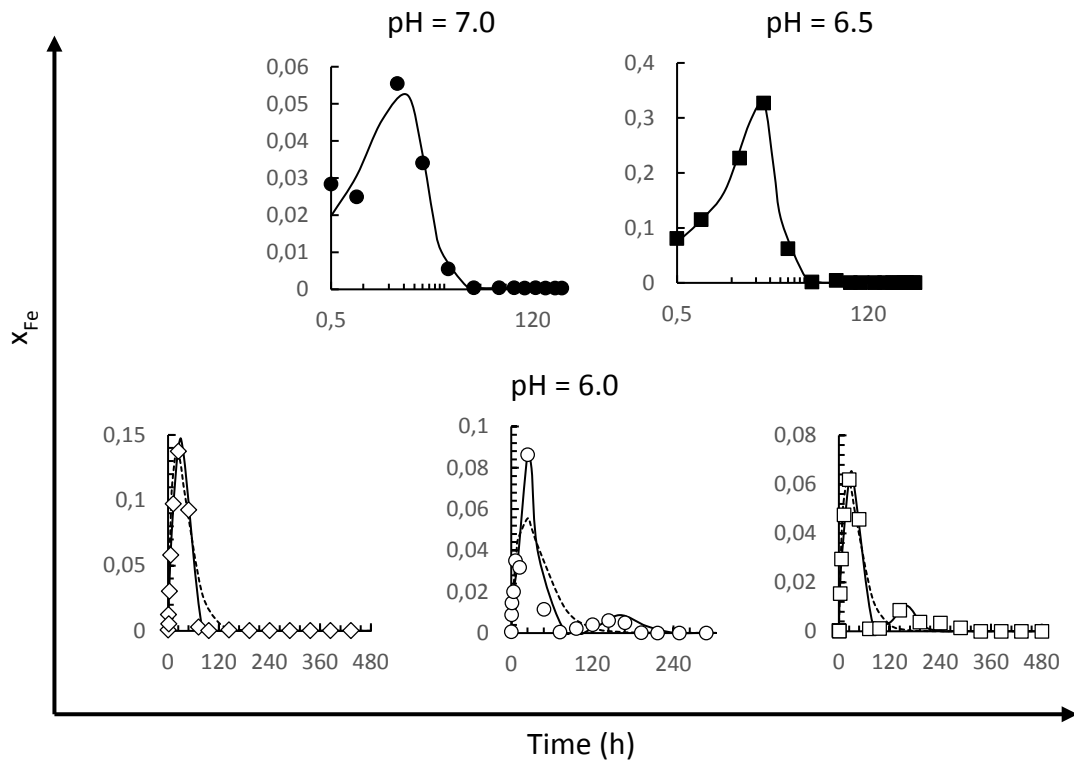


Fig. 8. Fe release ( $x_{\text{Fe}} = [\text{Fe}]/[\text{Fe}]_0$ ) over time at pH values under study, where  $[\text{Fe}]$  is the dissolved concentration of Fe and  $[\text{Fe}]_0$  is the maximum Fe concentration that can be released from the sediment. Experimental release (● pH=7; ■ pH=6.5; ◇ pH=6.0,  $[\text{Fe}]_{\text{seawater}}=9.02 \mu\text{g/L}$ ; ○ pH=6.0,  $[\text{Fe}]_{\text{seawater}}=46.1$



602  $\mu\text{g/L}$ ; and  $\square$  pH=6.0,  $[\text{Fe}]_{\text{seawater}}=153 \mu\text{g/L}$ ) and simulated curves are represented: —most suitable model  
603 for each assay; ---Martín-Torre et al. (2015b) model applied to assays at pH=6.0.

604  
605  
606

Table 5. Estimated values for the maximum concentrations of Fe that can be released from the reduced ( $[\text{FeRed}]_0$ ) and oxidised ( $[\text{FeOx}]_0$ ) sediment fractions and kinetic rate coefficients in all assays.

<b>pH</b>	<b>[Fe]<sub>seawater</sub></b> <b>(µg/L)</b>	<b>[FeRed]<sub>0</sub></b> ——— <b>(mg/kg)</b> ———	<b>[FeOx]<sub>0</sub></b>	<b>k<sub>1,Fe</sub></b>	<b>k<sub>2,Fe</sub><sup>0</sup></b>	<b>k<sub>2,Fe</sub><sup>1</sup></b>	<b>k<sub>3,Fe</sub><sup>0</sup></b>	<b>k<sub>3,Fe</sub><sup>1</sup></b>	<b>k<sub>1,a</sub></b>	<b>k<sub>2,a</sub></b>	<b>k<sub>3,a</sub></b>
								(h <sup>-1</sup> )			
7.0	6.80	276	39.0	1.08 10 <sup>-4</sup>	2.74 10 <sup>-1</sup>	---	2.95 10 <sup>-1</sup>	---	---	---	---
6.5	3.50	86.0	623	3.50 10 <sup>-4</sup>	2.01 10 <sup>-1</sup>	---	2.35 10 <sup>-1</sup>	---	---	---	---
6.0	9.02	42.8	8040	1.88 10 <sup>-3</sup>	1.42 10 <sup>-2</sup>	1.11 10 <sup>-1</sup>	9.73 10 <sup>-2</sup>	0	1.16 10 <sup>-2</sup>	1.15 10 <sup>-2</sup>	6.95 10 <sup>-4</sup>
6.0	46.1	26.1	6620	1.88 10 <sup>-3</sup>	1.09 10 <sup>-2</sup>	1.37 10 <sup>-1</sup>	1.32 10 <sup>-1</sup>	7.61 10 <sup>-2</sup>	1.71 10 <sup>-2</sup>	1.72 10 <sup>-2</sup>	1.62 10 <sup>-3</sup>
6.0	153	58.6	18400	1.88 10 <sup>-3</sup>	9.90 10 <sup>-3</sup>	4.12 10 <sup>-2</sup>	1.69 10 <sup>-1</sup>	6.80 10 <sup>-2</sup>	1.89 10 <sup>-2</sup>	1.89 10 <sup>-2</sup>	1.52 10 <sup>-3</sup>

607  
608  
609  
610  
611

### 4.3. Trace element modelling at pH=6.0

The contaminant release at pH=6.0 is first simulated according to the kinetic scheme used at higher pH values (Eq. 3). However, the release reaction is influenced by the dissolved Fe concentration so the rate coefficient  $k_{2,i}$  is modified according to Eq. 15 to account for this effect.

$$k_{2,i} = k_{2,i}^0 + \frac{k_{2,i}^1}{x_{Fe}} \quad (15)$$

where  $i$  represents the element (Zn, Pb, Ni, Cd, or As),  $k_{2,i}^0$  and  $k_{2,i}^1$  are kinetic rate coefficients, whereas the fraction of Fe released from the sediment is defined as  $x_{Fe} = \frac{[Fe]}{[FeS]_0}$  with  $[Fe]$  being the dissolved concentration of Fe and  $[FeS]_0$  being the maximum concentration of Fe that can be released from the sediment. The former coefficient ( $k_{2,i}^0$ ) considers the characteristics of the aqueous medium that might modify the solubility of the different species present in the sediment whereas  $k_{2,i}^1$  represents the direct influence of Fe on the release rate.

Including the influence of Fe, the simulated results of Zn and Cd fit well with their experimental release. However, the simulated release of Pb, Ni and As (not shown) is much lower than the experimental one for short periods ( $t < 96$  h) so the ionic competition with other cations should be considered in a similar way as the Fe release.

To avoid a high increase in the number of parameters, only the influence of Zn, which is the major trace element in the studied sediment, is also included when simulating the release of Pb, Ni and As. Hence, a further term is added and the rate coefficient of the

release reaction of Pb, Ni and As includes the combined influence of Fe and Zn as shown in Eq. 16.

$$k_{2,i} = k^0_{2,i} + \frac{k^1_{2,i}}{x_{Fe}} + \frac{k^2_{2,i}}{x_{Zn}} \quad (16)$$

where i represents the element (Pb, Ni and As),  $k^2_{2,i}$  is the rate coefficient which represents the direct influence of Zn on the release rate and the fraction of Zn released from the sediment is defined as  $x_{Zn} = \frac{[Zn]}{[ZnS]_0}$  with [Zn] being the concentration of dissolved Zn and  $[ZnS]_0$  being the maximum concentration of Zn that can be released from the sediment. The variables  $k^0_{2,i}$ ,  $k^1_{2,i}$  and  $x_{Fe}$  were previously explained.

The fit between the simulated and experimental release for the different assays at pH=6.0 when using this modified model is shown in Fig. 7 with continuous lines. The percentage variation-explained values ( $R^2$ ) for the different assays at pH=6.0 are, from the lowest to the highest concentrations of Fe in the seawater, 99.5, 96.1 and 96.3. These values are influenced by the simulated release of Fe, leading to higher  $R^2$  values of elemental release for the better Fe fittings.

The concentrations of each element in the reduced and oxidised sediment fractions are estimated by using this modified model and are listed in Table 3. At pH=6 and  $[Fe]_{seawater}=9.02 \mu\text{g/L}$ , the estimated concentrations take the same value as they do when using the model by Martín-Torre et al. (2015b). Similar to what occurred at most neutral pH values, higher concentrations are released from the reduced fraction than from the oxidised fraction of the sediment, except the Ni and As in the assay in which the seawater contains  $46.1 \mu\text{g/L}$  of Fe.

Regarding the pH=6 assay with the lowest seawater Fe concentration (9.02 µg/L), a better fitting is obtained when using the modified model than the previous one. Percentage variation-explained values ( $R^2$ ) of 99.5, 98.6, 99.7, 98.4 and 81.2 instead of 99.3, 98.4, 98.3, 97.0 and 74.1 are obtained for Zn, Pb, Cd, Ni and As, respectively. However, a trade-off between the estimated work and the accuracy should be decided by the user because the use of this modified model implies the estimation of more parameters.

Given that ionic competition, based on the different solubility products, is a process with a great influence on the contaminant release, the interactions among all of the ions could be added through additional elemental fractions ( $x_{Pb}$ ,  $x_{Cd}$ ,  $x_{Ni}$  and  $x_{As}$ ). This approach has been attempted, and despite the increasing the number of estimated parameters, the results do not present enough sensitivity to better fit the experimental release. Hence, the dependence of Fe is considered for all the studied trace elements at pH=6.0, but the influence of Zn is only contemplated for Pb, Ni and As release at this pH value.

Something similar occurs when this model, which was proposed for the simulation of contaminant release at pH=6.0, is used to fit experimental results from assays at pH values of 7.0 and 6.5 a better fit is obtained when the parameters that are not included in the initial proposed model employ a value of zero.

As expected, higher concentrations of the studied trace elements are released from the sediment ( $[MS]_{i,0} = [MOx]_{i,0} + [MRed]_{i,0}$ ) at lower pH values because of the greater

solubility of the studied contaminants at acidic pH values, except for As, which presents the highest mobilisation at pH=6.5 (Fig. 9 a). In comparing the mobilisation at pH=6.0, Fig. 9b indicates that the higher Fe concentrations in the selected seawater causes a slightly higher mobilisation of all the studied contaminants.

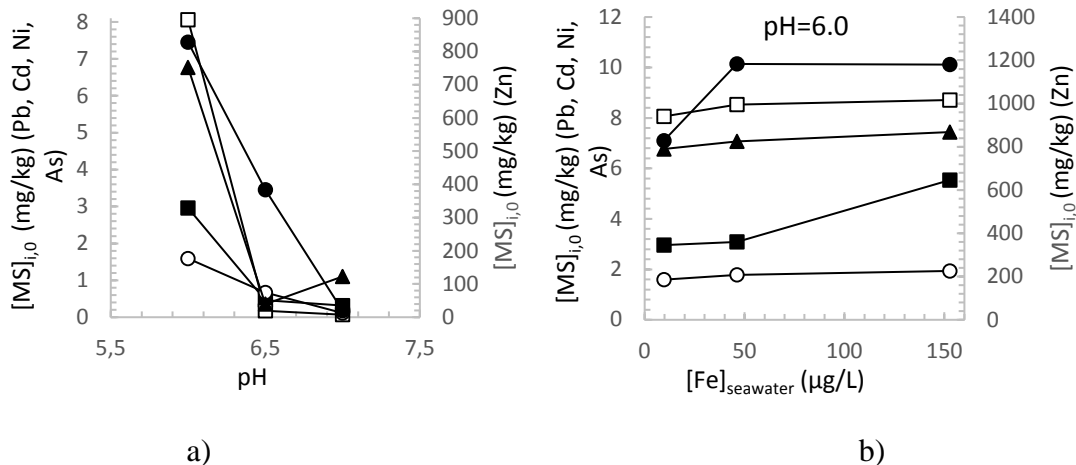


Fig. 9. a) Maximum concentration of contaminant that can be released from the sediment as a function of pH; and b) maximum concentration of contaminant that can be released from the sediment at pH=6.0 as a function of the Fe concentration in the seawater. ● Zn; ■ Pb; ○ Ni; □ Cd; and ▲ As

As previously stated, the rate coefficients of the different assays are presented in Table 4, in which As is the only element with an adsorption or precipitation reaction ( $k_3 \neq 0$ ). Moreover, at pH=6.0 the oxidation and adsorption/precipitation processes of this oxyanion do not depend on the initial Fe concentration in the seawater, and thus the rate coefficients have the same value in the three assays conducted at this pH value.

Although the model considers the influence of Zn on the release of Pb, Ni and As, it takes a nonzero value ( $k_{2,i}^2 \neq 0$ ) in all the cases for Ni release, for Pb release at the two highest concentrations of Fe in seawater (153 and 46.1 µg/L) and for As mobilisation at  $[Fe]_{seawater} = 46.1$  µg/L; this last case likely occurs because the released concentration of this oxyanion from the oxidised fraction is higher than it was from the reduced fraction

at this seawater Fe content. However, the obtained rate kinetic parameters ( $k^0_{2,i}$ ,  $k^1_{2,i}$  and  $k^2_{2,i}$ ) do not present a clear trend as a function of  $[\text{Fe}]_{\text{seawater}}$ .

The type of acidification ( $\text{CO}_2$  or  $\text{HNO}_3$ ) used in the pH-static assay influences the rate coefficients obtained from the Martín-Torre et al. model (2015b). Contrary to what occurs when the mineral acid is used (Martín-Torre et al., 2015b), rate coefficients obtained using  $\text{CO}_2$  do not present a clear trend with respect to the pH and cannot be fitted to any polynomial equation.  $\text{HNO}_3$  is a strong oxidising acid that generates soluble salts in the medium, and it might be completely dissociated.  $\text{CO}_2$  is a weak oxidising acid that forms partial insoluble salts, the solubility products of which modify the characteristics of the medium through ionic competition and therefore influence the element release rates.

The maximum concentrations of the elements that can be released from the sediment might depend on the type of acidification in addition to the oxidation state of the sediment. Hence, higher values are generally obtained in assays that employ  $\text{CO}_2$  instead of  $\text{HNO}_3$  (Martín-Torre et al., 2015b). Exceptions to this trend are Pb concentration at pH values of 7.0 and 6.5 (similar values are independent of the selected acid) and As at the most neutral pH values, where higher concentrations are released from the sediment in assay samples acidified by  $\text{HNO}_3$ .

The parity plots with the percentage variation-explained values ( $R^2$ ) and relative standard deviation (RSD) included a consideration of the global modified model of this work for all the assays performed, as obtained for each contaminant (Fig. 10). Parity plots are useful for the validation of the model in terms of the released element

729 concentration at any time and pH value. In general, at release higher than 25% of the  
730 maximum dissolved concentration, differences between experimental and simulated  
731 mobilisation are lower than 20% although a higher dispersion is observed in the case of  
732 As. Better fittings are obtained at pH values of 7.0 and 6.5 because of a lack of ~~the~~  
733 influence from the Fe concentration and ionic competition on the elemental release. The  
734 percentage variation-explained values ( $R^2$ ) for each contaminant are higher than 97.8 for  
735 all the elements under study, except for As, in which  $R^2=89.4$ . The high values of this  
736 statistical parameter show the good fit of the proposed model.



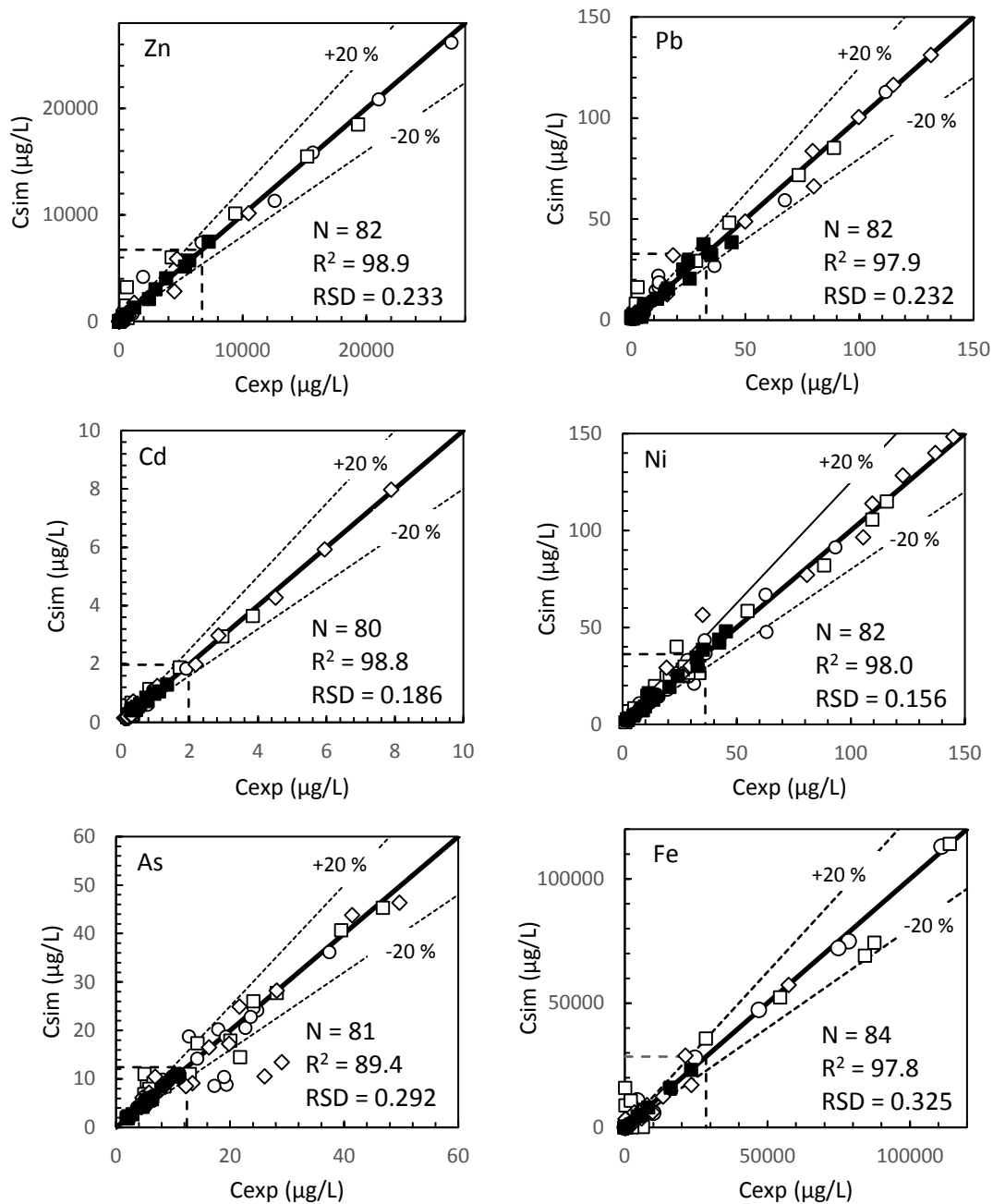


Fig. 10. Parity plots of the element concentrations from the experiment (C<sub>exp</sub>) and simulated results (C<sub>sim</sub>) of the elements under study. The area inside the dashed square includes concentrations lower than 25% of the maximum dissolved concentration. ● pH=7.0; ■ pH=6.5; ◇ pH=6.0, [Fe]<sub>seawater</sub>=9.02 µg/L; ○ pH=6.0, [Fe]<sub>seawater</sub>=46.1 µg/L; and □ pH=6.0, [Fe]<sub>seawater</sub>=153 µg/L. Additionally, the data number (N), percentage variation-explained value (R<sup>2</sup>) and relative standard deviation (RSD) are shown.

## 5. CONCLUSIONS

This work presents the experimental results of Zn, Pb, Cd, Ni, Cr, Cu and As mobilisation over time when sediment and seawater are totally mixed and acidified by

CO<sub>2</sub> gas in a pH-static leaching test. Long-term 480-h leaching tests are performed at pH values of 7.0, 6.5 and 6.0 to assess different levels of acidification.

The evolution of the redox potential and Fe release over time at pH=6.0 is different than the evolution at the more neutral pH values under study. Therefore the influence of the seawater Fe concentration is assessed by conducting assays at pH=6.0 using natural seawater with different Fe contents: 9.02; 46.1 and 153 µg/L.

A set of three in-series reactions for trace elements, for Fe and for other ions associated with Fe is proposed to model a Fe/multi-ion-dependent mechanism for trace metal release. The model uses global R<sup>2</sup> values of 98.9-89.4 and RSD < 0.325 to explain the release behaviour over time for Zn, Pb, Cd, Ni and As at pH values of 7.0, 6.5 and 6.0, which mimic the potential CCS acidification, and three seawater iron concentrations, which represent estuarine seawater in the iron mine areas.

The model proposed in this work extends the scope of previous models to the acidification of seawater with CO<sub>2</sub>, at different iron concentrations; however, a trade-off between estimation and accuracy is made because there are higher numbers of parameters in the proposed model. Using the Aspen Custom Modeler, the maximum concentrations of each element that can be released from the sediment, and the kinetic rate coefficients are estimated for all the cases.

Additionally, the kinetic rate coefficients obtained in this work are compared with those that were obtained previously when HNO<sub>3</sub> was used to acidify the medium. Different trends are observed because of the impact that CO<sub>2</sub> has on the ionic competition and

contaminant release, highlighting that the displacement reactions should be considered when acidification from CO<sub>2</sub> leakages originating from CCS sites is assessed.

The parity plots of the pH-static leaching test when using CO<sub>2</sub> to acidify the medium show a good fit between the experimental and simulated element release, confirming that the proposed model can be applied to simulate contaminant mobilisation from contaminated sediment to seawater under total mixed acidic conditions at pH values of 7.0, 6.5 and 6.0. Hence, a useful, broader generalised kinetic model that explains the contaminant release over time in sediment-seawater mixtures that were acidified by HNO<sub>3</sub> or CO<sub>2</sub> was made to obtain acidic pH values and different concentrations of iron. The proposed model is flexible enough to work with sediments that have different contaminant contents through model-fitting parameters such as the oxidised and reduced fractions and the kinetic rate coefficients.

## Acknowledgements

This work was financially supported by the Spanish Ministry of Economy and Competitiveness, Project CTM 2011-28437-C02-01, ERDF included. M.C. Martín-Torre was funded by the Spanish Ministry of Economy and Competitiveness by means of F.P.I. fellowship No. BES-2012-053816.

## References

- Appelo, C.A.J., Drijver, B., Hekkenber, R., de Jonge, M. 1999. Modeling in situ iron removal from groundwater. *Groundwater* 37 (6), 811-817.
- Appelo, C. A. J., van der Weiden, M. J. J., Tournassat, C, Charlet, L. 2002. Surface complexation of ferrous iron and carbonate on ferrihydrite and the mobilization of arsenic. *Environ. Sci. Technol.*, 36, 3096-3103. DOI: 10.1021/es010130n
- Arai, Y., Sparks, D. L., Davis, J.A. 2004. Effects of dissolved carbonate on arsenate adsorption and surface speciation at the hematite-water interface. *Environ. Sci. Technol.* 2004, 38, 817-824. DOI: 10.1021/es034800w

- Ardelan, M. V., Steinnes, E., Lierhagen, S., Linde, S. O. 2009. Effects of experimental CO<sub>2</sub> leakage on solubility and transport of seven trace metals in seawater and sediment. *Sci. Total Environ.* 407 (24), 6255-6266. DOI: 10.1016/j.scitotenv.2009.09.004
- Ardelan, M. V., Steinnes, E. 2010. Changes in mobility and solubility of the redox sensitive metals Fe, Mn and Co at the seawater-sediment interface following CO<sub>2</sub> seepage. *Biogeosciences*, 7, 569–583. DOI: 10.5194/bg-7-569-2010
- Basallote, M.D., de Orte, M.R., del Valls, T.A., Riba, I. 2014. Studying the effect of CO<sub>2</sub>-induced acidification on sediment toxicity using acute amphipod toxicity test. *Environ. Sci. Technol.* 48, 8864-8872. DOI: 10.1021/es5015373
- Bateman, K., Turner, G., Pearce, J.M., Noy, D. J., Birchall, D., Rochelle, C. A. 2005. Large-Scale Column Experiment: Study of CO<sub>2</sub>, porewater, rock reactions and model test case. *Oil Gas Sci. Technol.*, Vol. 60 (1), 161-175.
- BOE, 2008. Resolution of 28 November 2007, vol. 34. Spanish Ministry of Industry, Tourism and Trade, Madrid, Spain, pp. 7099-7102.
- Cahill, A. G. and Jakobsen, R. 2015. Geochemical modeling of a sustained shallow aquifer CO<sub>2</sub> leakage field study and implications for leakage and site monitoring. *Int. J. Greenh. Gas Con.* 37, 127–141. DOI: 10.1016/j.ijggc.2015.03.011
- Cappuyns, V., Swennen, R. and Verhulst, J. 2004a. Assessment of acid neutralizing capacity and potential mobilisation of trace metals from land-disposed dredged sediments. *Science of the Total Environment*, 333 (1-3), 233- 247. DOI: 10.1016/j.scitotenv.2004.05.007
- Cappuyns, V., Swennen, R. and Devivier, A. 2004b. Influence of ripening on pH<sub>stat</sub> leaching behaviour of heavy metals from dredged sediments. *Journal of Environmental Monitoring* 6 (9), 774-781. DOI: 10.1039/B406672C
- Cappuyns, V., Swennen, R. 2005. Kinetics of element release during combined oxidation and pH<sub>stat</sub> leaching of anoxic river sediments. *Appl. Geochem.* 20, 1169–1179. DOI : 10.1016/j.apgeochem.2005.02.004
- Cappuyns, V. and Swennen, R. 2008. The application of pH<sub>stat</sub> leaching tests to assess the pH-dependent release of trace metals from soils, sediments and waste materials. *J. Hazard. Mater.* 158(1), 185-195. DOI: 10.1016/j.jhazmat.2008.01.058
- CEN/TS 14997. 2015. Characterization of waste - Leaching behaviour tests – Influence of pH on leaching with continuous pH-control.
- Centioli, D., Comans, R.N.J., Gaudino, S., Galas, C., Belli, M. 2008. Leaching tests: useful tools for the risk assessment of contaminated sediments. *Annali dell'Istituto Superiore di Sanità* 44 (3), 252-257.
- Coz, A., González-Piñuela, C., Andrés, A., Viguri, J.R. 2007. Physico-chemical and environmental characterisation of sediments from Cantabria estuaries (Northern Spain). *Aquat. Ecosyst. Health*, 10, 41-46. DOI: 10.1080/14634980701212118

- De Orte, M. R., Sarmiento, A. M., Basallote, M. D., Rodríguez-Romero, A., Riba, I., del Vallas, A. 2014. Effects on the mobility of metals from acidification caused by possible CO<sub>2</sub> leakage from sub-seabed geological formations. *Sci. Total Environ.* 470-471, 356-363. DOI: 10.1016/j.scitotenv.2013.09.095
- Di Toro, D., Mahony, J. D., Hansen, D. J., Scott, K. J., Hicks, M. B., Mayr, S. M., Redmond, M. 1990. Toxicity of cadmium in sediments: the role of acid volatile sulfide. *Environ. Toxicol. Chem.* 9, 1487–1502. DOI: 10.1002/etc.5620091208
- Eggleton, J. and Thomas, K.V. 2004. A review of factors affecting the release and bioavailability of contaminants during sediment disturbance events. *Environ. Int.* 30(7), 973-980. DOI: 10.1016/j.envint.2004.03.001
- Frye, E., Bao, C., Li, L., Blumsack, S. 2012. Environmental Controls of Cadmium Desorption during CO<sub>2</sub> Leakage. *Environ. Sci. Technol.*, 46, 4388–4395. DOI: 10.1021/es3005199
- Hering, J. G. and Stumm, W. 1990. Oxidative and reductive dissolution of minerals. In *Mineral-Water Interface Chemistry*, vol. 23 (eds. M. F. Hochella and A. F. White), 427–465. *Reviews in Mineralogy and Geochemistry*. Mineralogical Society of America.
- Hoffman, E.L. 1992. Instrumental neutron activation in geoanalysis. *J. geochem. Explor.* 44, 297-319. DOI: 10.1016/0375-6742(92)90053-B
- Horckmans, L., Swennen, R., Deckers, J. 2007. Retention and release of Zn and Cd in spodic horizons as determined by pHstat analysis and single extractions. *Sci Total Environ.* 376, 86–99. DOI: 10.1016/j.scitotenv.2007.01.077
- Hwang, K.-Y., Kim, H.-S., and Hwang, I. 2011. Effect of Resuspension on the Release of Heavy Metals and Water Chemistry in Anoxic and Oxic Sediments. *Clean – Soil, Air, Water* 39 (10), 908–915. DOI: 10.1002/clen.201000417
- Intergovernmental Panel on Climate Change (IPCC) (2014) *Climate change 2014: mitigation of climate change*. In: Working Group III of the Intergovernmental Panel on Climate Change.
- Ishimatsu, A., Kikkawa, T., Hayashi, M., Lee, K.-S., Kita, J. 2004. Effects of CO<sub>2</sub> on marine fish: larvae and adults. *J. oceanogr.* 60, 731-741. DOI: 10.1007/s10872-004-5765-y
- Jain, A., Loeppert, R.H. 2000. Effect of competing anions on the adsorption of arsenate and arsenite by ferrihydrite. *J. Environ. Qual.* 29 (5), 1422–1430. DOI: 10.2134/jeq2000.00472425002900050008x
- Johnston, S.G. , Morgan, B., Burton, E.D. 2016. Legacy impacts of acid sulfate soil runoff on mangrove sediments: Reactive iron accumulation, altered sulfur cycling and trace metal enrichment. *Chem. Geol.* 427 (1), 43–53. DOI: 10.1016/j.chemgeo.2016.02.013

- Kikkawa, T., Kita, J. and Ishimatsu, A. 2004. Comparison of the lethal effect of CO<sub>2</sub> and acidification on red sea bream (*Pagrus major*) during the early developmental stages. *Mar. Pollut. Bull.* 48, 108–110. DOI: 10.1016/S0025-326X(03)00367-9
- Kirsch, K., Navarre-Sitchler, A. K., Wunsch, A., McCray, J. E. 2014. Metal Release from Sandstones under Experimentally and Numerically Simulated CO<sub>2</sub> Leakage Conditions. *Environ. Sci. Technol.* 48, 1436–1442. DOI: 10.1021/es403077b
- Lawter, A., Qafoku, N. P., Wang, G., Shao, H., Brown, C. F. 2016. Evaluating impacts of CO<sub>2</sub> intrusion into an unconsolidated aquifer: I. Experimental data. *Int. J. Greenh. Gas Con.* 44, 323–333. DOI: 10.1016/j.ijggc.2015.07.009
- Little, M.G., Jackson, R.B. 2010. Potential impacts of leakage from deep CO<sub>2</sub> geosequestration on overlying freshwater aquifers. *Environ. Sci. Technol.*, 44, 9225–9232. DOI: 10.1021/es102235w
- Lu, J., Partin, J. W., Hovorka, S. D., Wong, C. 2010. Potential risks to freshwater resources as a result of leak-age from CO<sub>2</sub> geological storage: a batch-reaction experiment. *Environ. Earth Sci.* 60 (2), 335–348. DOI: 10.1007/s12665-009-0382-0
- Luther III, G.W., Kostka, J.E., Church, T.M., Sulzberger, B., Stumm, W. 1992. Seasonal iron cycling in the salt-marsh sedimentary environment: the importance of ligand complexes with Fe(II) and Fe(III) in the dissolution of Fe(III) minerals and pyrite, respectively. *Mar. Chem.* 40, 81–103. DOI: 10.1016/0304-4203(92)90049-G
- Martín-Torre, M.C., Payán, M.C., Verbinen, B., Coz, A., Ruiz, G., Vandecasteele, C., Viguri, J.R. 2015a. Metal release from contaminated estuarine sediment under pH changes in the marine environment. *Arch. Environ. Contam. Toxicol.* 68(3), 577–587. DOI: 10.1007/s00244-015-0133-z
- Martín-Torre, M.C., Ruiz, G., Galán, B., Viguri, J.R. 2015b. Generalised mathematical model to estimate Zn, Pb, Cd, Ni, Cu, Cr and As release from contaminated estuarine sediment using pH-static leaching tests. *Chem. Eng. Sci.* 138, 780–790. DOI: 10.1016/j.ces.2015.08.053
- Meng, X.G., Bang, S.B., Korfiatis, G.P. 2000. Effects of silicate, sulfate, and carbonate on arsenic removal by ferric chloride. *Water Res.* 34, 1255–1261. DOI: 10.1016/S0043-1354(99)00272-9
- Meng, X., Korfiatis, G.P., Bang, S., Bang, K. 2002. Combined effects of anions on arsenic removal by iron hydroxides. *Toxicol. Lett.* 113, 103–111. DOI: 10.1016/S0378-4274(02)00080-2
- Millero, F.J., Sotolongo, S., Izaguirre, M. 1987. The oxidation kinetics of Fe(II) in seawater. *Geochim. Cosmochim. Ac.* 51, 793–801.
- Millero, F.J. and Izaguirre, M. 1989. Effect of ionic strength and ionic interactions on the oxidation of Fe(II). *J. Solution Chem.* 18 (6), 585–599.

- 957 Millero, F. J., Yao, W. and Aicher, J. 1995. The speciation of Fe(II) and Fe(III) in  
958 natural waters. *Mar. Chem.* 50 (1-4), 21–39. DOI: 10.1016/0304-4203(95)00024-L  
959
- 960 Millero, F. J. 2009. Thermodynamic and Kinetic Properties of Natural Brines. *Aquat.*  
961 *Geochem.* 15 (1), 7-41. DOI: 10.1007/s10498-008-9053-0  
962
- 963 Morse, J. W. and Arakaki, T. 1993. Adsorption and coprecipitation of divalent metals  
964 with mackinawite (FeS). *Geochim. Cosmochim. Ac.* 57 (15), 3635-3640. DOI:  
965 10.1016/0016-7037(93)90145-M  
966
- 967 Omoregie, E. O., Couture, R.-M., van Cappellen, P., Corkhill, C. L., Charnock, J. M.,  
968 Polya, D. A., Vaugahn, D., Vanbroekhoven, K., Lloyd, J. R. 2013. Arsenic  
969 Bioremediation by Biogenic Iron Oxides and Sulfides. *Appl. Environ. Microb.* 79 (14),  
970 4325-4335. DOI: 10.1128/AEM.00683-13  
971
- 972 Payán, M.C., Galan, B., Coz, A., Vandecasteele, C., Viguri, J.R. 2012a. Evaluation  
973 through column leaching tests of metal release from contaminated estuarine sediment  
974 subject to CO<sub>2</sub> leakages from Carbon Capture and Storage sites. *Environ. Pollut.* 171,  
975 174-184. DOI:10.1016/j.envpol.2012.07.029  
976
- 977 Payán, M.C., Verbinnen, B., Galan, B., Coz, A., Vandecasteele, C., Viguri, J.R., 2012b.  
978 Potential influence of CO<sub>2</sub> release from a carbon capture storage site on release of trace  
979 metals from marine sediment. *Environ. Pollut.* 162, 29–39. DOI:  
980 10.1016/j.envpol.2011.10.015  
981
- 982 Payán, M.C., Galan, B., Ruiz, G., Coz, A., Viguri, J.R. 2013. Pb and Zn release from  
983 intertidal marine sediment in contact with acidified CO<sub>2</sub> seawater: Mathematical model  
984 for column leaching tests. *Chem. Eng. Sci.* 95, 85–93. DOI: 10.1016/j.ces.2013.02.059  
985
- 986 Rodríguez-Romero, A., Basallote, M. D., De Orte, M. R., Delvalls, T. Á., Riba, I.,  
987 Blasco, J. 2014. Simulation of CO<sub>2</sub> leakages during injection and storage in sub-seabed  
988 geological formations: Metal mobilization and biota effects. *Environ. Int.* 68, 105–117.  
989 DOI: 10.1016/j.envint.2014.03.008  
990
- 991 Root, R.A., Dixit, S., Campbell, K. M., Jew, A.D., Hering, J. G. and O'Day, P.A. 2007.  
992 Arsenic sequestration by sorption processes in high-iron sediments. *Geochim.*  
993 *Cosmochim. Ac.* 71, 5782-5803. DOI: 10.1016/j.gca.2007.04.038  
994
- 995 Salomons, W. 1995. Long-term strategies for handling contaminated sites and large-  
996 scale areas. In: Salomons, W. and Stigliani, W. M. (Eds.), *Biogeodynamics of*  
997 *Pollutants in Soils and Sediments (Risk assessment of delayed and non-linear*  
998 *responses)*, Springer, Berlín (Germany), 1-30. ISBN: 3-530-58732-2  
999
- 1000 Schwertmann, U. 1991. Solubility and dissolution of iron oxides. *Plant Soil* 130 (1), 1–  
1001 25.  
1002
- 1003 Shtiza, A., Swennen, R., Cappuyns, V., Tashko, A. 2009. ANC, BNC and mobilization  
1004 of Cr from polluted sediments in function of pH changes. *Environ. Geol.* 56(8), 1663-  
1005 1678. DOI: 10.1007/s00254-008-1263-7  
1006

- Sigg, L. 2000. Redox potential measurements in natural waters: significance, concepts and problems. In: Schulz, H.D., Fischer, W.R., Böttcher, J., Duijnisveld, W.H.M. (Eds.), Redox Fundamentals, Processes and Applications. Springer, Berlin, pp. 1–12.
- Thamdrup, B. 2000. Bacterial manganese and iron reduction in aquatic systems. *Adv. Microb. Ecol.* 16, 41–84.
- Tokoro, C., Yatsugi, Y., Koga, H., Owada, S. 2010. Sorption Mechanisms of Arsenate during Coprecipitation with Ferrihydrite in Aqueous Solution. *Environ. Sci. Technol.* 44 (2), 638–643. DOI: 10.1021/es902284c
- Vaca-Escobar, K., Villalobos, M., Pi-Puig, T., Zanella, R. 2015. Approaching the geochemical complexity of As(V)-contaminated systems through thermodynamic modelling *Chem. Geol.* 410, 162–173. DOI: 10.1016/j.chemgeo.2015.06.007
- Wallmann, K., Petersen, W., Reiners, C., Gramm, H. 1996. Trace element diagenesis in polluted sediments of the river Elbe estuary. In: Calmano, W. and Förstner, U. (Eds.), Sediments and toxic substances (Environmental effects and ecotoxicity), Berlin (Germany), 197–213. ISBN: 3-540-60051-5
- Van Herreweghe, S., Swennen, R., Cappuyns, V., Vandecasteele, C. 2002. Chemical associations of heavy metals and metalloids in contaminated soils near former ore treatment plants: a differentiated approach with emphasis on  $\text{pH}_{\text{stat}}$ -leaching. *J. Geochem. Explor.* 76 (2), 113–138. DOI: 10.1016/S0375-6742(02)00232-7
- Wang, G., Qafoku, N.P., Lawer, A.R., Bowden, M., Harvey, O., Sullivan, C., Brown, C.F. 2016. Geochemical impacts of leaking CO<sub>2</sub> from subsurface storage reservoirs to an unconfined oxidizing carbonate aquifer. *Int. J. Greenh. Gas. Con.* 44, 310–322. DOI: 10.1016/j.ijggc.2015.07.002
- Wong, V.N., Johnston, S.G., Burton, E.D. Bush, R.T, Sullivan, L.A., Slavich, P.G. 2013. Seawater-induced mobilization of trace metals from mackinawite-rich estuarine sediments. *Water Res.* 47(2):821–32. DOI: 10.1016/j.watres.2012.11.009
- Zhang, G.-S., Qu, J.-H., Liu, H.-J., Liu, R.-P., Li, G.-T. 2007. Removal Mechanism of As(III) by a Novel Fe–Mn Binary Oxide Adsorbent: Oxidation and Sorption. *Environ. Sci. Technol.* 41 (13), 4613–4619. DOI: 10.1021/es063010u
- Zheng, L., Apps, J. A., Zhang, Y., Xu, T., Birkholzer, J. T. 2009. On mobilization of lead and arsenic in groundwater in response to CO<sub>2</sub> leakage from deep geological storage. *Chem. Geol.* 268, 281–297. DOI: 10.1016/j.chemgeo.2009.09.007
- Zheng, L., Qafoku, N. P., Lawter, A., Wang, G., Shao, H., Brown, C. F. 2016. Evaluating impacts of CO<sub>2</sub> intrusion into an unconsolidated aquifer: II. Modeling results. *Int. J. Greenh. Gas Con.* 44, 300–309. DOI: 10.1016/j.ijggc.2015.07.001